SPE/IADC-223713-MS

System for Real-Time Rate of Penetration Optimization Using Machine Learning with Integrated Preventive Safeguards Against Hole Cleaning Issues and Stick-Slip

T. S. Robinson, Exebenus, Sugar Land, TX, United States; P. Mohammed Arshad and O. E. Revheim, Exebenus, Stavanger, Norway; M. Regan, Exebenus, Dubai, United Arab Emirates; P. Bekkeheien, Exebenus, Sugar Land, TX, United States

This paper was prepared for presentation at the SPE/IADC International Drilling Conference and Exhibition held in Stavanger, Norway, 4 – 6 March 2025.

Abstract

Drilling related costs can contribute 30-70% of operators' capital expenditures for well construction. To reduce costs, operators can reduce bit-on-bottom time and flat time. This work describes a drilling optimization advisory system utilizing machine learning (ML) with integrated safeguards for preventing issues that might occur following drilling parameter changes intended to increase rate of penetration (ROP), such as hole cleaning (HC) issues which might lead to stuck pipe, or stick-slip that reduces drilling efficiency.

This work builds on the authors' previous publications on ROP optimization (OTC-31680-MS, SPE-214521-MS), incorporating modules targeted at prompt detection of stick-slip for timely mitigation, and ensuring advised drilling parameter changes do not potentially cause HC issues and pack-offs. The HC safeguard utilized a downhole Equivalent Circulating Density (ECD) estimation ML model (SPE-208675-MS), queried by the optimizer to estimate effects of proposed drilling parameter changes, and corresponding ROP, on the ECD. A configurable tolerance to (expected) ECD changes from baseline parameters ensured any ECD increases were acceptable. The stick-slip detector monitored the frequency spectra of surface rotary speed and torque measurements, and utilized a classifier to estimate the probability of stick-slip symptoms' presence.

The ROP optimization system with integrated ECD safeguard has been field-deployed in SE Asia since Q4 2023, with no stuck pipe incidents relating to pack-offs occurring since this version of the software has been in use. The further enhanced version with integrated stick-slip detection was deployed to field operations in Q2 2024; analysis of historical well data with torsional vibration issues demonstrates the detector identifies stick-slip with high performance, achieving a precision of 0.92 on holdout (unseen) drilling data intervals from five wells, with all stick-slip symptoms present in the data identified. With stick-slip identified based on the estimated probabilities, human monitoring staff are notified, and the ROP

optimizer automatically alters its behavior to allow torsional vibrations to be mitigated in order to maintain high drilling efficiencies.

The Literature contains many works on the separate topics of stuck pipe prevention, ROP optimization and vibration mitigation, however these have not previously been incorporated into a holistic system balancing these different, sometimes competing, objectives. This work demonstrates effective integration of modules for ROP optimization, and detection of pack-off risks and torsional vibrations, into a combined system enabling increased drilling efficiency while reducing risks leading to non-productive time, contributing to overall reduced well construction time.

Introduction

Drilling operations in hydrocarbon wells are expensive activities, representing a large component of capital expenditures in the upstream oil and gas industry. Typical daily operating costs during the drilling phase can range from several tens of thousands to well in excess of a million US Dollars, with rig rates contributing a large portion of this in deepwater operations where semi-submersibles or drillships are hired. Analysis by IHS Markit and the US Energy Information Administration (EIA) estimated that drilling contributes 30-40% of total well costs for onshore wells, and ~60% of total well costs for offshore deepwater wells, although offshore costs vary considerably depending on the specifics of the well (U.S. EIA 2015). As a result, operators are incentivized to improve drilling efficiency and rate of penetration (ROP). In addition to faster drilling reducing bit-on-bottom time, mitigation of drilling dysfunctions (such as vibration), and prevention of drilling incidents resulting in non-productive time, are crucial for reducing operational time and hence overall well construction costs. However, these goals may be at odds with each other in many scenarios; for example, increasing the ROP also increases the rate at which cuttings are produced, which in turn increases the risk of poor hole cleaning if there is insufficient fluid circulation to remove these cuttings. Subsequently, pack-offs and stuck pipe incidents may occur, often resulting in extensive non-productive time and resources spent on freeing the drill string. Similarly, torsional vibration (stick-slip) is a commonly encountered dysfunction that reduces drilling efficiency (energy is transferred into oscillations of drillstring or bottom-hole assembly (BHA) rather than into penetrating the formation) and can lead to damage to expensive downhole equipment if not mitigated promptly. Hence, effective drilling optimization requires a holistic approach balancing faster drilling with risk avoidance and mitigation, in order to achieve an optimal outcome of safe, fast, and efficient drilling leading to reduced well construction time.

ROP optimization using machine learning (ML) techniques has been an actively researched topic in recent years, with many works published on ROP prediction. Junca Rivera et al. (2022) described a methodology utilizing Deep Learning for improving ROP in various drilling environments, though this work was focused more on offline offset well analysis and planning for future wells, rather than real-time applications. Methodologies based on optimizing multiple objectives have been described by Singh et al. (2022) and Zhang et al. (2023), for example by attempting to simultaneously maximize ROP while minimizing Mechanical Specific Energy. Other published works utilized sophisticated but computationally-expensive methods for finding optimal sets of drilling parameters, for example metaheuristic algorithms such a Particle Swarm Optimization or Genetic Algorithms (Cao et al. 2022, Erge et al. 2022, Fernandez Berrocal et al. 2022, Nautiyal and Mishra 2023), which again hinders their usage for real-time optimization. However, only a few of the published ROP optimization methodologies and systems have been field-tested on multiple wells, in different fields, with published results demonstrating efficacy (Singh et al. 2022, Robinson 2022a, Robertson et al. 2023, Al-Riyami 2023, Singh et al. 2024). A paper by Hai et al. (2024) described field testing of an ROP optimization system in China on a single well. Achieving good ROP prediction results is insufficient for proving the efficacy of an optimization system, which must be done in the field by actioning system-generated advice (and assessing the ROP observed in response), either

indirectly by the rig crew after being notified by monitoring specialists (Al-Riyami 2023), or using a closed-loop optimization workflow, an example of which has been published by Singh et al. (2024).

Other applicability limitations described in the literature include formation or field-specific models (Batruny 2019, Safarov et al. 2022, Elahifar 2024, Jiao et al. 2024), and the use of input variables associated with particular downhole apparatus. An example of this is differential pressure, which was demonstrated by Singh et al. to be an effective predictor for ROP and controllable parameter when drilling with positive displacement motors (Singh et al. 2019, Singh et al. 2021). However, this does not apply to drilling with rotary steerable systems (RSS) which are increasingly commonly used. Another example could be the use of downhole measurements in methodologies for detection drilling dysfunctions such as torsional vibrations (Singh et al. 2022, Robertson et al. 2023), which imposes requirements to use specific downhole tools during operations. Wang et al. (2024) have published work on an ROP prediction methodology dependent on formation data obtained by coring. All of the aforementioned limitations reduce the scope in which these methods can be used, introduce pre-project work requirements for customizing models to a specific field or set of formations, or increase costs of operation through requiring expensive downhole tools.

In this work, the authors describe a software system and methodology for optimizing the ROP in real-time during drilling operations, while maintaining operational safety using multiple safeguarding modules integrated with the ROP optimizer. The optimization system described in this work utilizes sub-systems for detection of stick-slip symptoms and prevention of hole cleaning issues in order to dynamically determine operational boundary thresholds, however the system architecture is modular by design, and can be readily extended with new modules addressing other known drilling dysfunctions. The ROP optimizer and safeguards utilize a suite of generalized ML models that use only readily-available real-time surface-measured data as inputs. "Generalized" in this context refers to models that have been designed and *pre-trained* for immediately deployable and effective "global" usage, thus avoiding restrictions to their scope to specific regions, fields, formations or wells with available local offset data. This enables them to be used out-of-the-box on unfamiliar wells that were not used during the model development and training process. This approach is intended to replicate usage in the field on a new well. The use of only surface data at inference time, and no downhole measurements, is intended to prevent dependencies on any particular downhole tools, enable system outputs to be generated in real-time, and to maximize the number of drilling operations in which the system could be readily used.

Prior to introducing the safeguarding modules described in this work, an earlier version of the system (Robinson 2022a) was used in the field since 2021, with detailed field testing results obtained from an ultra-deepwater well and a shallow water well, located in West Africa and Malaysia respectively, available in a previous paper (Al-Riyami et al. 2023). The successful outcomes of these field trials and proven operational value provided the context for the methodological updates and extended field-usage reported in this work.

Methods and processes

The main focus of this section concerns the integration of multiple component modules into a (usually cloud-based) holistic system that considers multiple objectives, namely selecting drilling parameters for increased ROP, monitoring estimated downhole ECD changes in response to higher ROP, and real-time detection of torsional vibration symptoms. Each system could be run independently to fulfil their design objectives, however collective usage within an integrated system was expected to provide greater operational value than the sum of their parts. This is due to automated actions that can be taken by the optimization system when aware of a broader operational context, for example proactively avoiding potential hole cleaning issues, or shifting focus from increasing ROP to dysfunction-mitigation upon detection of stick-slip symptoms as they initially manifest.

The ROP optimization system utilizes a core module for identifying candidate combinations of drilling parameters that are expected to maximize ROP, subject to certain constraints to safeguard the operation.

These limits may be user-configured at any point before or during operations (based on rig constraints for example), actively determined during operations through scenario modelling, or alternatively derived from real-time risk detection methods for identifying drilling dysfunctions. The core optimization module used was an updated version of system described by the authors in a previous paper, using an updated ML model for ROP estimation, and a similar directed multi-stage parameter sweep in order to select an optimal combination of drilling parameters (Robinson 2022a).

The two classes of safeguarding modules integrated with the core optimizer, can be broadly described as "*reactive safeguards*" and "*preventive safeguards*". Within this framework, reactive safeguards monitor real-time or historical data for prompt detection of drilling dysfunction symptoms, and publish a severity metric to human users or other software systems to support mitigating actions to be taken, either by appropriate staff or automatically. The stick-slip symptom detection module linked to the optimization system is an example of a reactive safeguard. Preventive safeguards attempt to estimate the potential impact of proposed drilling parameter changes on other key parameters relating to operational safety, drilling dysfunctions or events leading to non-productive time through scenario modelling. This enables the optimizer to pro-actively avoid potentially consequential issues by imposing dynamic safety limits based on the current operational context. In the context of this work, the preventive safeguard is intended to protect against issues with poor hole cleaning, which can result in pack-offs and costly non-productive time stemming from stuck pipe incidents. This is achieved through modelling the downhole Equivalent Circulating Density (ECD) changes expected from various scenarios with modified drilling parameters, due to increases in ECD being an indicator of poor hole cleaning that is commonly monitored by practitioners in the field. This built on the authors' prior work on ECD modelling using ML techniques (Robinson 2022b). With faster drilling, the excess cuttings produced and suspended in the drilling fluid contribute to increasing the average density of the circulating fluids.

Overview of the ROP optimization system

An overview of the cloud-based ROP optimization system, its component modules, and how these integrate with remote data infrastructure, is shown in Fig. 1. The system consists of an orchestrator module responsible for:

- receiving and pre-processing data from the remote data store (WITSML stores were connected to in this work),
- passing pre-processed data to, and requesting drilling parameters from, the core ROP optimizer,
- receiving data from the support modules (safeguards) used for detecting drilling risks in real-time.

In addition to the orchestrator and core ROP optimizer, two safeguarding modules were used to augment the optimization system. The first was a reactive safeguard performing real-time drilling dysfunction detection to identify possible drivers of reduced drilling efficiency, for example torsional vibrations (stick-slip) or other vibrations. Once detected, the information shared with the orchestrator could prompt the system to either pause attempts to identify drilling parameters for maximizing ROP until the dysfunction is mitigated or continue issuing drilling parameter advice as normal, configured according to users' preferences. Alternatively, the system could be extended to issue advice for mitigation, however this was outside of the scope of this work. The second module, a preventive safeguard, used an ML model to estimate the expected effect of changing drilling parameters, with respect to downhole ECD increases and potential risk of poor hole cleaning. Information from this scenario analysis was then used to constrain the drilling parameter advice.

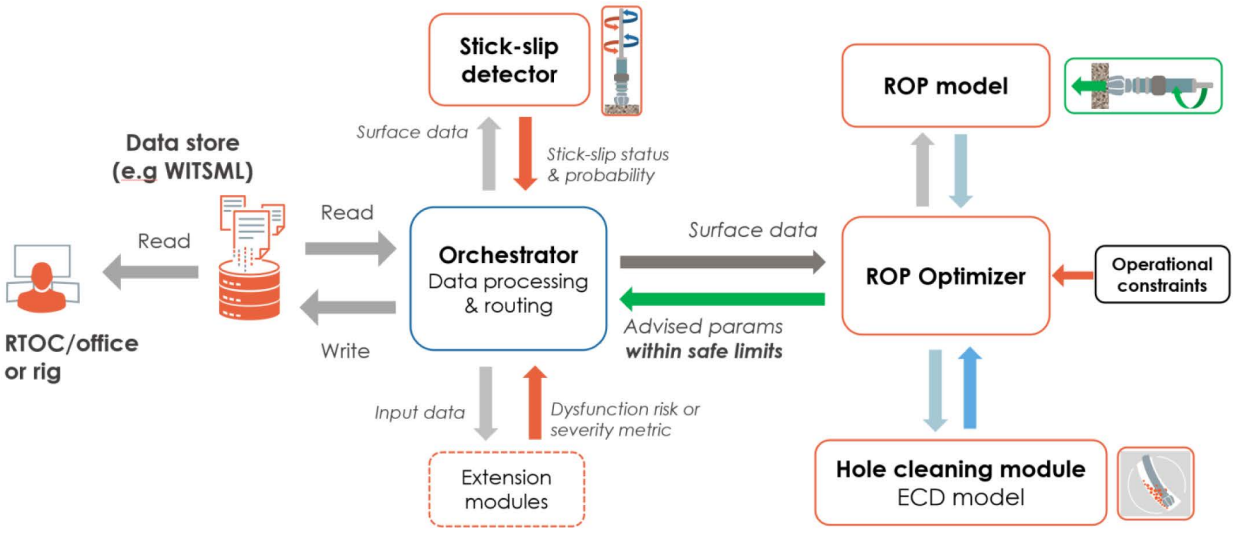

Figure 1—Overview of the drilling rate-of-penetration optimization system with integrated safeguarding modules. The architecture is extensible by design, with the capability for other dysfunction detection or scenario modelling modules to be integrated with the orchestration module.

The core optimizer module identifies the weight-on-bit (WOB) and surface rotary speed values that maximize the expected ROP provided by the ROP model, subject to a set of safety constraints required to avoid drilling dysfunctions, hole cleaning issues, or equipment damage. These limits can be user-defined ahead of or during operations, for example based on the rig constraints or equipment manufacturer's recommended safe operating limits. Alternatively, these can be determined dynamically based on a preventive safeguard, in this case focused on risks of poor hole cleaning through modelling the downhole ECD expected in response to drilling parameter and ROP changes. Furthermore, information published by the stick-slip detector (and reactive safeguarding modules more generally) to the orchestrator can be used to alter the system's behavior, shifting focus from increasing ROP to mitigating identified drilling dysfunctions.

All sub-systems that involve modelling – for ROP estimation, ECD estimation and stick-slip symptom detection - utilize generalized pre-trained ML models developed using only surface-measured data as inputs, given its routine availability in drilling operations, to support widespread and scalable usage of the system. These models are trained and validated using data from independent wells, hence are not limited by design in their utility to specific fields, regions, formation types, BHA or bit types, or intervals within a particular well. These characteristics allow the system to be used directly on new and unfamiliar wells, without the need for pre-project customization of models, which would require additional upfront effort and hinder useability. The ROP optimization system was used in the scope of this project in an advisory capacity, although it could be readily modified to integrate with a rig control system for closed-loop drilling parameter optimization. The optimization system's architecture is extensible by design, and could be augmented with additional modules for providing protection against different drilling dysfunctions, for example lateral and axial vibration, or equipment failures which could include drillstring buckling or damage to drill bits/cutters, RSS, downhole logging tools, or mud motors.

Hole cleaning (ECD) safeguard

Background on ECD modelling techniques. *The following background discussion on ECD, and context for modelling it using ML approaches, is a condensed version of introductory material from the authors' previously published work on this topic* (Robinson 2022b). Various factors influence the downhole ECD, such as drilling mud characteristics (density, viscosity, and flow rate into the well), the quantity and granularity of cuttings in suspension, well pressure and temperature (Rommeveit 1997), drillstring rotary speeds (Hemphill 2008, Ahmed 2010, Kulkarni 2017), and gains and losses. Hence, modelling ECD is a

complex and inherently multivariate problem. A detailed discussion of factors affecting ECD is provided by Pål Skalle in *Drilling Fluid Engineering*, Section 7 (Skalle 2010). Usually, companies rely on expensive downhole sensors to measure ECD, which typically provide data at lower sampling frequencies relative to the surface measurements, and require data to be transmitted up to the surface. Most of these tools have operational limitations (e.g. related to pressure and temperature) which might prevent their use throughout the whole operation. In practice, ECD is typically obtained by measuring the pressure loss P_s in the annulus using a quartz gauge pressure sensor, and then applying the following formula:

$$ECD = C\frac{P_s}{D_{TV}} + \rho_{mud}, \quad (1)$$

where D_{TV} is the true vertical depth (TVD), ρ_{mud} is the mud density, and C is a constant. If using units of ppg, psi and ft for mud density, annular pressure loss and TVD respectively, then $C = {}^{1}/_{0.052}$, yielding a commonly used version of this formula. Eq. 1 is also used in conjunction with hydraulics calculations, which estimate values for P_s instead of using measurements from a downhole tool. Examples of rheological models commonly used for hydraulics calculations in the industry include Bingham-Plastic, Power-Law and Herschel-Bulkley (Whittaker 1985). These calculations typically require many input parameters, which can be challenging to obtain values for, increasing the configuration effort required to use them and the potential variability in results with respect to these parameters. Furthermore, they make certain assumptions, for example when calculating pressure drop using Bingham-Plastic and Power-Law models, laminar flow of drilling fluids is assumed, as well as the drillstring being located concentrically in a circular hole, no drillstring rotation, and that the drilling fluid is incompressible (Bourgoyne 1991). These assumptions may not hold well in reality; laminar flow is typically associated with low pumping rates, and drillstring rotation is routine in many operations where ECD monitoring is of interest. These limitations provide clear motivation for developing alternative numerical methods for estimating ECD, which has led to publication of various works applying ML to this problem (Abdelgawad 2019, Alkinani 2019, Al Saihati 2021a, Al Saihati 2021b, Gamal 2021).

Integration of ECD estimation into the ROP optimization process. The hole cleaning safeguard module was built around an ML model for estimating downhole ECD, using only the surface-measured data and the (ML model-estimated) ROP as inputs. This method allows various scenarios to be modelled before making changes to drilling parameters, in order to prevent a drilling hazard from occurring, in this case poor hole cleaning or cuttings accumulation. This ML model, an updated version of the model described in a previous work by the authors (Robinson 2022b), was pre-trained on a curated historical dataset with globally-distributed wells, which included surface data and downhole ECD measurements. The model did not have design assumptions limiting its scope to a specific set of regions, fields, formations, or downhole equipment configurations.

The process used by the ROP optimizer when integrated with the hole cleaning safeguard is shown in Fig. 2. After receiving a request from the orchestrator for drilling parameter advice, the core optimizer generates a set of possible candidate solutions (combinations of drilling parameters) in which to search for an optimum. The optimizer then filters these candidates according to configured safety constraints on the allowed ranges of WOB, rotary speed, and mud flow rates, and requests estimates for ROP values corresponding to each candidate solution from the ROP model. A second filter is then applied based on maximum allowed ROP.

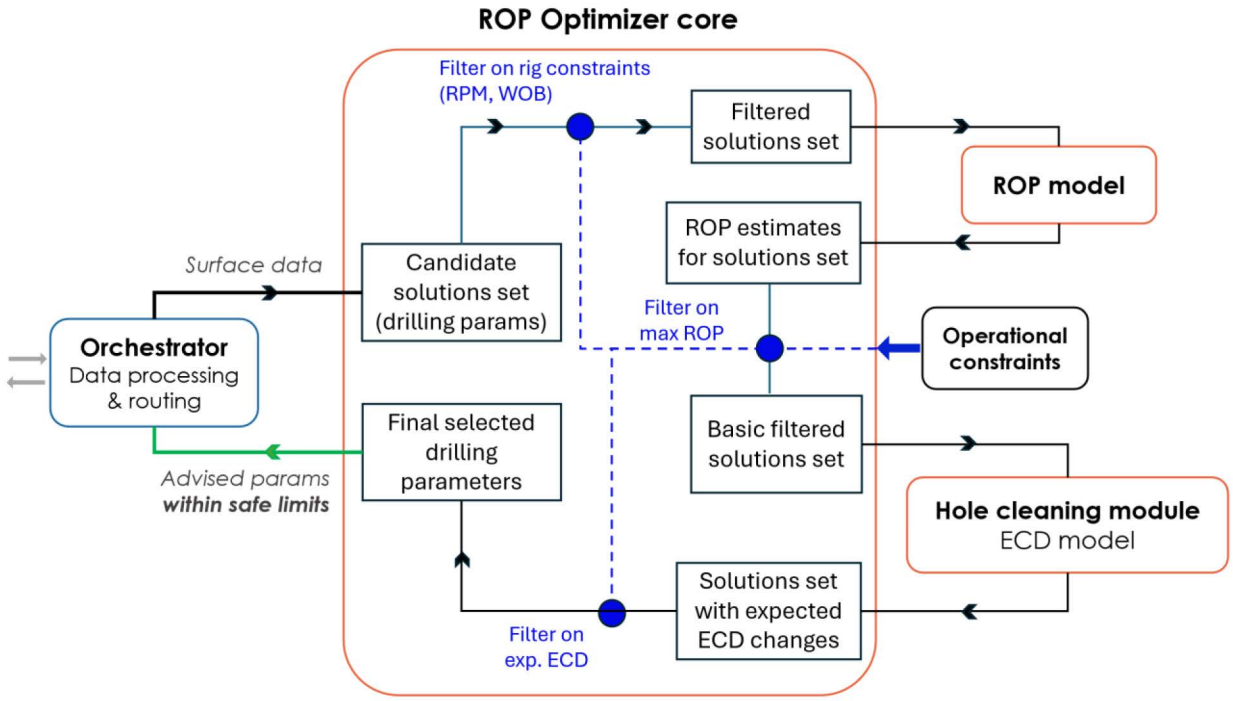

Figure 2—Process diagram describing how the ROP optimizer works using a preventive hole cleaning safeguarding module, that estimates downhole ECD under different scenarios associated with candidate combinations of surface drilling parameters (WOB and rotary speed).

After these ROP estimates within the configured search range are obtained from the ROP model, the ECD model is queried by the core optimizer to assess the expected impact of each candidate solution's proposed changes in drilling parameters (and corresponding ROP estimate) on the ECD. These are assessed relative to a "baseline" ECD estimate, which is defined to be the ECD value obtained by keeping the drilling parameters unchanged, after first generating a baseline ROP estimate from these. Based on the expected changes in ECD modelled for different scenarios, the potential risk of hole cleaning issues can be quantified, and a set of drilling parameters that are expected to keep ECD within a configured change tolerance can be selected from the set of possible candidate solutions. Candidate solutions expected to result in an ECD increase above the baseline value in excess of the configured safety threshold are consequently filtered out; when combined with the basic constraints applied earlier on, the optimal drilling parameters are then selected to be those that maximize ROP within the full set of safety limits. The optimum values are then returned by the core optimizer to the orchestrator, which then publishes outputs to the appropriate data store for consumption by end-users located in the real-time monitoring centers.

Stick-slip safeguard

Background on stick-slip detection methods. Given the detrimental impact of torsional vibrations on drilling efficiency and increased risk of equipment damage, it is unsurprising that modelling, detection and mitigation of these vibration issues is an actively researched topic in the drilling industry, with numerous published works. A common practice in the industry is to model stick-slip phenomena by treating the drillstring as a driven damped torsional oscillator, where the drive frequency is set by the drillstring/bit rotation and the damping force comes from the bit-rock interaction and friction forces acting on the drillstring from interaction with the borehole. This approach allows the natural frequencies of drillstrings, and their associated harmonics to be estimated based on the moment of inertia and torsion constant, which are calculated from the material and geometric properties of the tubulars and BHA. Guidance can then be issued to avoid driving the system at these frequencies and inducing a resonant interaction where energy is efficiently transferred into the torsional vibrations. Kamel et al. (2014) investigated physics-based methods

to model stick-slip when drilling with fixed-cutter bits, such as polycrystalline diamond compact (PDC) bits which are increasingly commonly used in the industry. The authors applied a lumped parameter method to obtain a dynamic model of the drilling system, and estimated equivalent system parameters estimated using a Lagrangian approach.

Another industry-standard approach utilizes downhole bit RPM measurements (or torque in some variations) to monitor stick-slip symptom severity. The following formula is applied to calculate a stick-slip severity index (SSI) for data from a particular time window:

$$SSI = \frac{\max(\omega_{bit}) - \min(\omega_{bit})}{2\bar{\omega}_{bit}}, \tag{2}$$

where ω_{bit} is the bit rotary speed, and $\bar{\omega}_{bit}$ denotes the mean bit rotary speed averaged over the time range. Although this approach has been used successfully across the industry to characterize stick-slip, it is dependent on downhole measurements, which must be up-linked via an appropriate telemetry method, which limits the rate at which this data can be consumed by monitoring systems. Examples of publications on stick-slip detection with methods using downhole data include the works of Pavone and Desplans (1994), Robnett et al. (1999), and Ledgerwood et al. (2010). The importance of the sampling rate of time series data used for vibration detection was studied by Srivastava et al. (2024), following on from Srivastava's work on stick-slip detection using ML (2022), who reported that while lower sampling rates could be used to detect torsional vibrations affecting the drillstring, a sampling rate of >10 Hz was recommended for optimum reliability with their method. While data at high sampling rates is available at the rig site directly from the sensors, data is typically down-sampled before transmission to remote data stores due to bandwidth limitations, hence any cloud-based stick-slip detection must still work reliably with 0.2 Hz to 1 Hz data to support general-purpose global usage.

Various works have applied ML techniques to the stick-slip detection problem; Gupta et al. (2019) reviewed the capability of various ML algorithms for predicting downhole vibrations from time-series data. Millan et al. (2019) described a methodology utilizing only surface data for characterizing drillstring vibrations in real-time. Similarly, Saadeldin et al. (2023) applied several ML algorithms with only surface measurements used for inference, to predict the severity of axial, torsional and lateral vibrations, where high frequency downhole measurements were used to determine vibration severities when training models. Sheth et al. (2022) described a method using surface measurements for predicting the stick-slip response for the next stand, from particular combinations of WOB and rotary speed values using a hybrid physics-guided machine learning methodology, to help drillers to proactively avoid drilling parameters likely to excite torsional vibrations. Another methodology combining physics-based and machine learning models was described by Yahia et al. (2024) for detecting stick-slip in real-time based on surface-measured data. The authors utilized sequences of time-series data and physical features (from a stiff-string torque and drag model) to construct a regression model predicting values of an SSI obtained from downhole measurements of bit RPM using Equation (2), although downhole measurements were not required at inference-time. A recurrent neural network with Long-Short Term Memory (LSTM) units was used to estimate the SSI directly from time-domain data, and a transfer learning approach was utilized to address challenges faced with generalization of the LSTM models.

Of relevance to the topic of this paper, researchers have combined stick-slip detection methodologies with ROP optimization systems. For example, Singh et al. (2022) developed a method for identifying stick-slip symptoms based on downhole measurements and filtering the space of candidate WOB and rotary speeds to avoid severe torsional vibrations, as part of a multi-component optimization objective considering ROP, Mechanical Specific Energy, and stick-slip, and reported on field test results from a system applying this technique (Robertson et al. 2023). Hai et al. (2024) also explicitly considered stick-slip and whirl as part of their methodology, by incorporating a full-scale drillstring dynamics model alongside a neural network for ROP prediction. Others have incorporated stick-slip detection into more broadly-focused systems using

an ensemble of machine learning models, such as neural networks with 1-D convolutions and attention mechanisms, for anomaly detection and dysfunction monitoring (Benzine et al. 2024).

Integration of real-time stick-slip symptom detection into the ROP optimization system. The key objective pertaining to real-time stick-slip detection in the context of this work was reliable and early detection, ideally during the onset phase, to support the operations teams in promptly mitigating the dysfunction to maintain drilling efficiency, and importantly before any equipment damage could occur. Predicting (hypothetical) combinations of WOB and drillstring rotary speeds most likely to induce stick-slip issues – a more challenging problem - was not in-scope nor necessary within the methodological framework presented. The detector identified stick-slip symptoms by monitoring the recent surface torque and rotary speed for characteristic patterns associated with torsional vibration. As only the readily available surface data was used, detection of High Frequency Torsional Oscillations (HFTO) affecting the BHA components was not within the scope of this work, as this would require downhole data acquired at much higher sampling rates than the surface measurements, which contradicted the key objective of developing a methodology and system utilizing only surface data. Hence, torsional vibrations affecting the drillstring were the primary focus of the stick-slip safeguard.

As vibrations are inherently periodic, an efficient workflow to identify vibration symptoms is to analyze time-series data from the rig in the frequency domain. This method is an extension of the authors' previously published work (Robinson 2023). Symptom severity can then be quantified based on an aggregated spectral representation of the data, using a pre-trained ML model. An example of this for torque is presented in Fig. 3(a), a 10 minute interval where the onset of torsional vibration symptoms was observed. In Fig. 3(b), the spectrum corresponding to the windowed signal is shown, following aggregation into a set of discrete spectral bands within a configured spectral range. As demonstrated previously by the authors in the context of automated detection of downlinking events via mud pulse telemetry (Robinson 2023), utilizing the spectral power densities associated with the various frequency bands as an input vector to a binary classification model is an effective method for detecting the periodic phenomenon of interest in real time. Many classification algorithms can provide probability estimates associated with the binary classes (symptom present / no symptom), which can in turn provide a proxy for the estimated symptom severity at a given point in time.

The aforementioned methodology was used to develop an ML model for detecting stick-slip symptoms, based on historical datasets from a set of wells in the North Sea, South America, and Southeast Asia, where intervals with stick-slip issues were present were labelled for each observation in time. Various models and algorithms could be used for classification in this context; in this work, the XGBoost (Chen 2016) package for ensembles of gradient-boosted decision trees was selected. The classification model's parameters were fitted on a subset of the data from a fixed set of wells, and was validated against data from another independent set of wells not used in training, to imitate real-world usage of the detection system in the field; further details on stick-slip detection performance are provided in the Results and Discussion section.

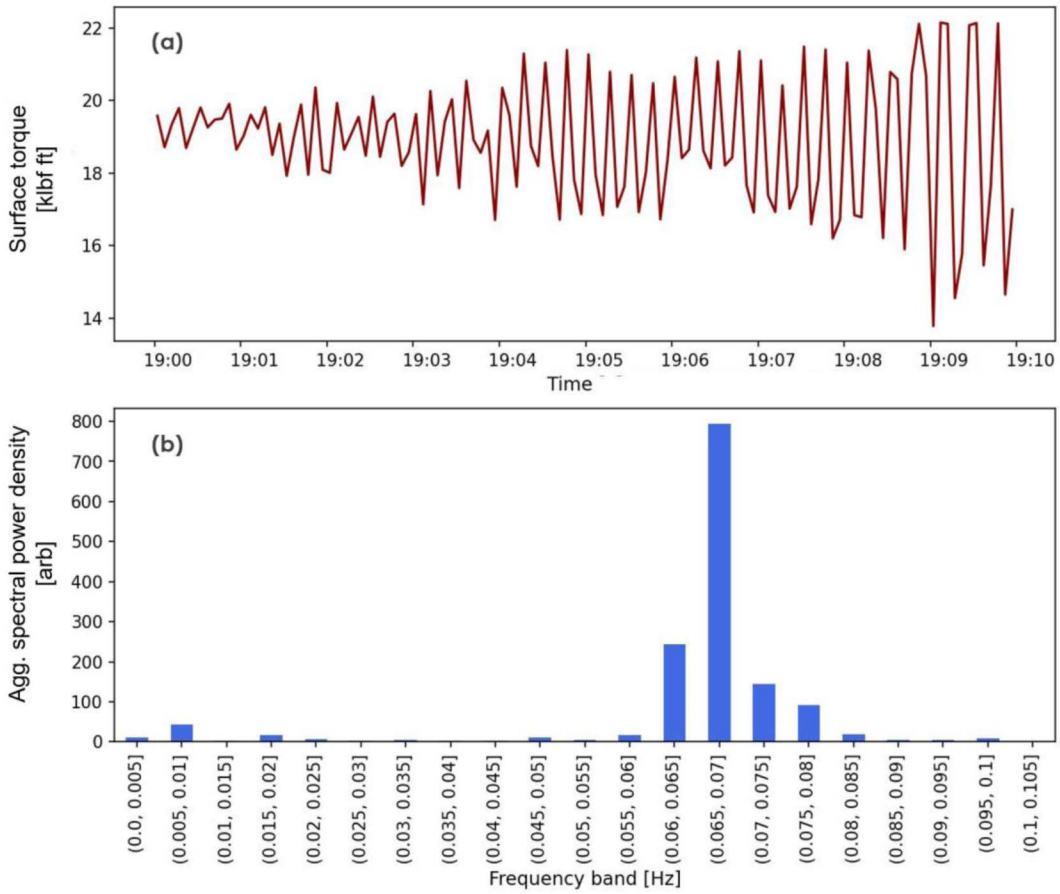

Figure 3—An example from an operation where torsional vibration symptoms were observed, with (a) a sample time-windowed torque signal from the operation, and (b) the corresponding spectral power densities aggregated into discrete frequency bands, which were used as inputs to the developed torsional vibration symptom detection system.

The process steps used by the stick-slip detection module, and its integration with the orchestrator module of the ROP optimization system and wider remote data infrastructure, are summarized in Fig. 4.

Surface torque and rotary speed data retrieved from the remote data store were sent by the orchestrator to the stick-slip safeguard module running in parallel. The detection module pre-processed the time-series data into windowed signals, which were then transformed into the frequency domain via Fast Fourier Transform methods to obtain power spectra. The maximum resolvable frequency of the calculated spectra is half the sampling frequency of the time-series according to Nyquist's Theorem, for example data sampled at 1 Hz will result in a upper limit of 0.5 Hz that can be resolved without issues with aliasing. Next, the power spectra were aggregated into discrete frequency bands, and preprocessed into the format expected by the ML classification model embedded into the detector. The system then requested probability estimates from the ML model for quantifying the risk from the drilling dysfunction. These were returned to the orchestrator after post-processing, which was then responsible for any actions required based on the information received.

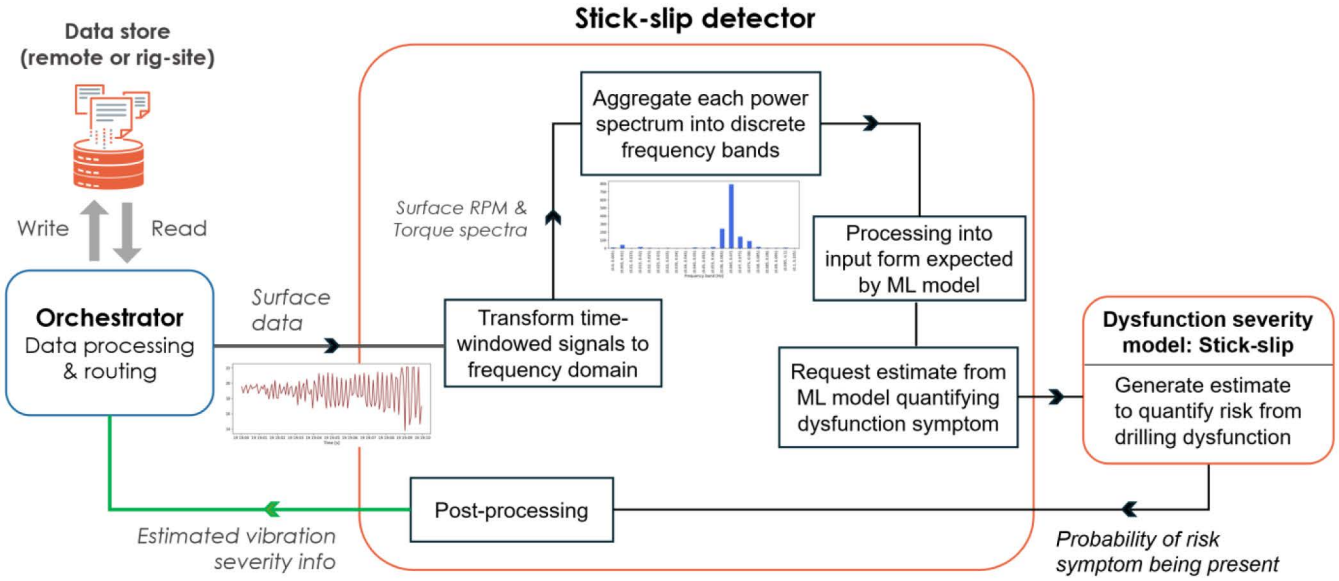

Figure 4—Process diagram for the stick-slip detection module integrated with the ROP optimization system as a reactive safeguard against drilling dysfunction. Reactive safeguards are integrated with the orchestrator module that controls whether the system requests advice for optimized drilling parameters. The sub-plots (a) and (b) from Fig. 3, displaying time-windowed surface data and an aggregated power spectrum are included here at the relevant stages of the detection process where they are utilized.

While it could be used independently for standalone drilling dysfunction detection purposes, the stick-slip safeguard was used in this work to ensure that drilling parameter recommendations generated by the ROP Optimization system do not compromise operational safety or pose risks to drilling equipment. Depending on the users' preferred tolerances to stick-slip symptom severity, the system interrupted the process for requesting advice for updated drilling parameters. An alternative strategy would be to extend the system to issue advice for mitigation, for example by recommending to follow industry-standard mitigation techniques involving reducing WOB and increasing drill string rotary speed, however this was not applied in this work.

A standard procedure used in the field by one of the operators is to follow ROP optimization advice only when there are no hole cleaning issues or drilling dysfunctions occurring, and when the ROP does not need to be controlled tightly for pressure management or wellbore stability purposes. The ROP optimizer has the capability to issue mud flow rate recommendations, however in typical operations this was restricted based on the operators' preferences, as constraints on the mud flow rate are usually determined by other factors outside of the remit of system.

Results and discussion

The ROP optimization system with integrated safeguards has been used in the field since November 2023, with a total of 76 wells utilizing the system to some degree at the time of writing. For certain wells, the system-generated advice was followed closely by the rig teams, whereas in other cases, the system was available to them but followed on a more ad-hoc basis due to other constraints related to controlling ROP. A geographic breakdown of the aforementioned 76 wells is provided in Table 1.

Table 1—Geographic summary of numbers of wells where the safeguarded ROP optimization system has been utilized in field operations.

REGION	WELL COUNT
Gulf of Mexico	8
Middle East	3
Caspian Sea	8
SE Asia	42
North Sea	3
S. America & Caribbean	7
Africa (East & SW)	5
TOTAL	**76**

Two main challenges were faced while assessing results for wells using the ROP optimization advisory system in routine field operations; firstly, time-depth curves for the wells comparing the planned time to reach total depth (TD) and the realized times were not available to the authors for analysis after concluding drilling. Similarly, time-depth curves for offset wells were not available. The second challenge was operators have competing requirements which must be satisfied during the drilling process, hence it is not reasonable to expect all drilling parameter advice to be implemented throughout. This obstructs a more comprehensive field results analysis, such as that provided in the authors' previous work for an ultra-deepwater well, where recommendations were actively followed throughout the drilling sections, with specific examples of increased ROP documented and where TD was reached 23 days ahead of the plan and ~2.5 days ahead of the expected technical limit (Al-Riyami et al. 2023). As a result, this limits the assessment to examining specific cases where drilling parameter advice was implemented by the rig teams, and any changes in ROP which could be attributed to these actions.

The remainder of this section will focus on 3 topics; (1) analyzing the impact observed on the ROP after following the optimization system's recommendations, (2) the performance of the downhole ECD estimation model embedded into a preventive safeguard module, and its impact in the field with respect to observed hole cleaning issues, and lastly (3) a selection of field case studies where the stick-slip safeguard successfully detected stick-slip symptoms in real-time on a variety of unfamiliar wells, and examples where the orchestrator appropriately interrupted the process for requesting drilling parameters to prioritize mitigating actions.

Impact on observed ROP in the field after implementing drilling parameter advice

In this sub-section, a variety of case studies where drilling parameter advice was followed are discussed with respect to the observed impact on ROP. Example offshore wells were selected from the Gulf of Mexico, Southeast Asia, and the North Sea, with a mix of deepwater and shallow water wells. Additional examples from the Middle East and Gulf of Mexico will be discussed in the sub-section discussing the results where the stick-slip safeguard in operations. The optimization system was used out-of-the-box in each of these cases, without specific pre-training to customize the system to the particular asset where the well was located. The first of these cases examined was located in the Gulf of Mexico, with a screenshot of drilling data visualized in a real-time WITSML viewer application shown in Fig. 5. The meanings of the various curves in the display are explained via the annotations added to the screenshot.

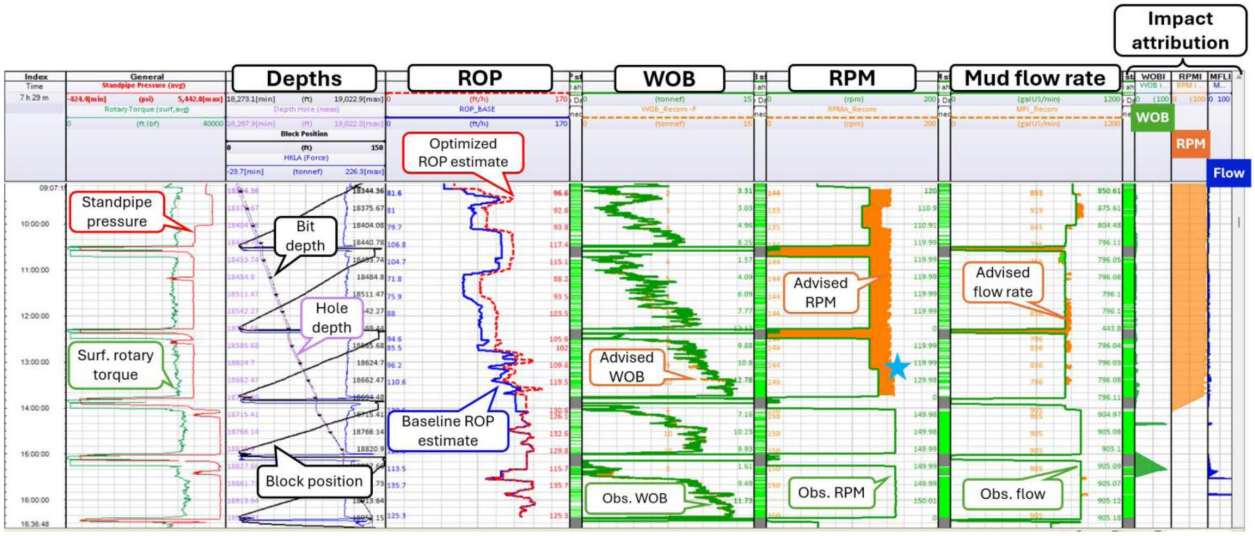

Figure 5—Screenshot from a commercial real-time data viewer application showing a Gulf of Mexico drilling case study using the ROP optimization system, where advised drilling parameter changes were implemented (increased rotary speed at the time indicated by blue star, in two stages), and higher ROP values observed, evidenced by the faster changes in block position in the second track from the left.

During this period of the operation, recommendations to increase rotary speed and slightly increase mud flow rates were provided by the optimizer. WOB was advised to be held mostly close to current values, though recommendations to slightly reduce WOB were provided in a few isolated cases towards the ends of the second and third stands after it had been steadily increased over the course of each stand. Rotary speed was increased in two stages, starting at the point marked by the blue star. Based on the change in steepness of the block position curve, it is evident that the ROP was increased for the two stands following the change. The penultimate stand in the image was actually drilled with a slightly lower WOB than the previous one, at value close to the optimizer's recommendations on the previous stand (orange "Advised WOB" curve), and was completed more quickly than the previous stands, in ~60 mins compared to ~80 mins on the stand immediately before, representing a ~25% reduction in time.

While drilling the 8.5 in. hole section of a deepwater well located in Southeast Asia, the operator recorded an example where drilling parameter advice provided by the ROP optimizer was explicitly implemented. For context, ROP was generally controlled in this well due to concerns around pore pressures, so advice for increasing ROP was only actioned in a few cases. A screenshot from a viewer application showing the drilling parameters and outputs from the ROP optimizer is provided in Fig. 6. Following discussions between monitoring specialists (who receive the ROP optimizer's outputs in an advisory capacity) and the Drilling Supervisor at the rig site, the rotary speed was increased from 120 rpm to the recommended 130 rpm. After the change, the ROP was observed to improve from 16 m/h to 25 m/h, representing an increase of ~56% in this particular case.

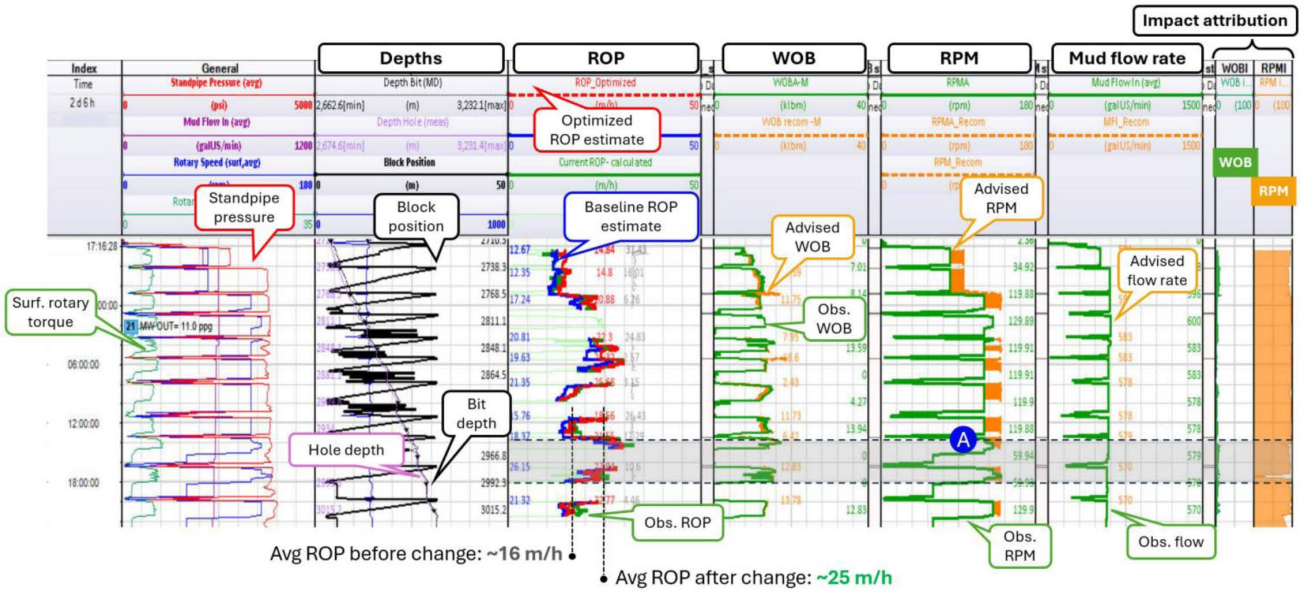

Figure 6—Example operation where drilling parameter advice to increase rotary speed provided by the ROP optimizer was communicated to the drilling supervisor and actioned at point (A), with increased ROP observed (green curve) during the shaded time interval.

In another shallow water well located in Southeast Asia drilled by the same operator, recommended drilling parameters were again implemented by the rig team following discussion with the drilling supervisor. During a casing-while-drilling operation for a 23 in. × 20 in. hole section, rotary speed was increased from 40 rpm to the advised 50 rpm, resulting in an observed improvement in average ROP from 45 m/h to 49 m/h, an increase of 8%. The higher RPM value was maintained for the next stand, with average ROP of 54 m/h observed (a total increase of 20% from 45 m/h), which corresponded well with the estimate for optimized ROP of 54.92 m/h generated by the ROP optimization system ahead of the rotary speed increase.

Shifting focus to a deepwater well in the North Sea, another scenario where rotary speed advice was followed, and attributed the highest expected impact by the optimizer, is presented in Fig. 7, a screenshot from a WITSML viewer, where the meanings of the various curves have been annotated. In the first two stands, the system recommends to increase rotary speed, and hold WOB steady. Based on the impact attribution curves (right-hand side of the screenshot), the optimizer prioritized rotary speed recommendations in importance over modifications to WOB.

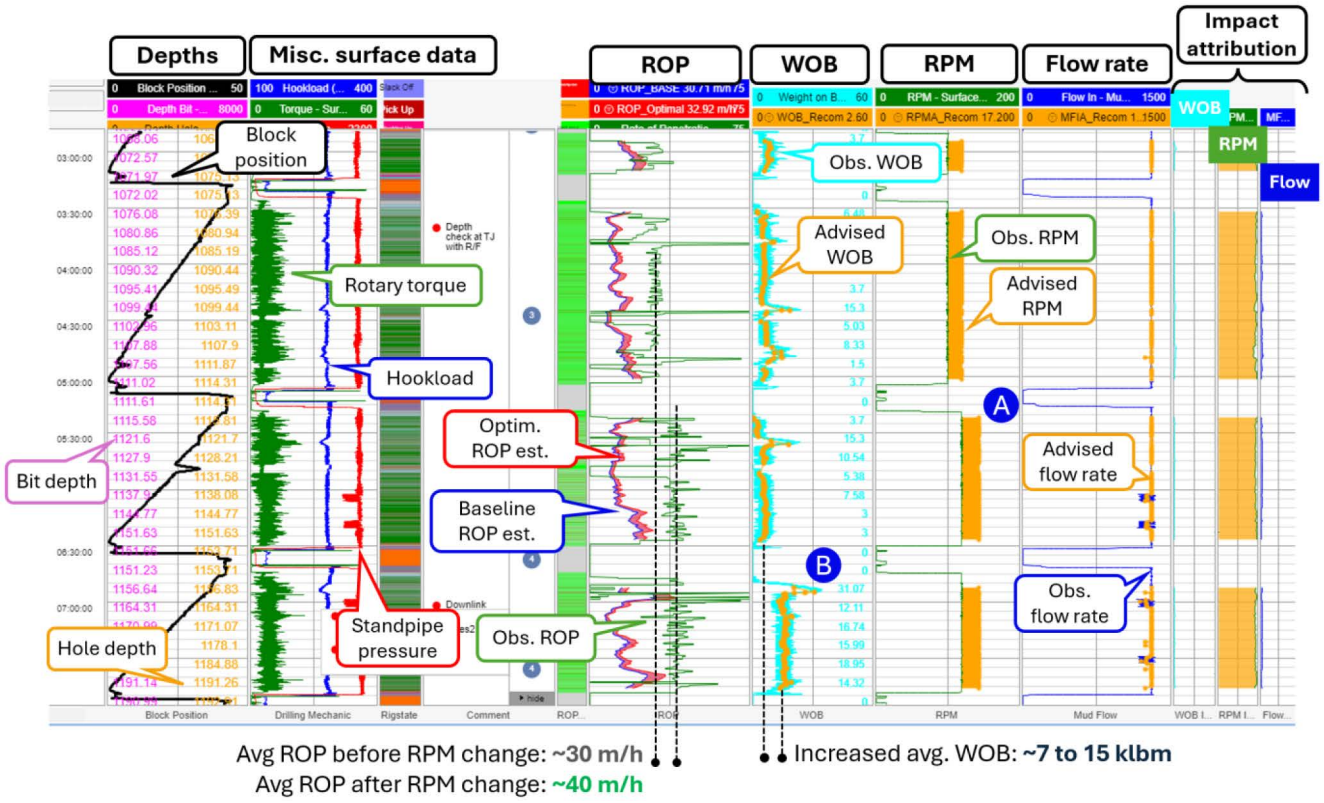

Figure 7—Example drilling scenario from a deepwater well located in the North Sea where drilling parameter advice to increase RPM was actioned by the rig team at point (A), after which the average ROP increased from ~30 m/h to ~40 m/h. As shown in the impact attribution history curves, the optimization system prioritized RPM increases over changes to WOB. At point (B), the WOB was increased, however little change in average ROP was observed, supporting the importances attributed by the software in this case.

At point (A) indicated in the figure, the decision was made to increase the rotary speed to approximately the level recommended by the optimizer on the previous two stands; this resulted in an increase in average ROP to ~40 m/h, compared to ~30 m/h on the previous stand drilled with lower RPM, as indicated by the green observed ROP curve. It should be noted in this case that the ML model underestimated the ROP with an approximately constant offset in this case, as can be seen by the baseline ROP estimates (blue curve), however the advised parameter changes appear to have been correctly identified, as demonstrated by the clear ROP increase achieved. Furthermore, the impact attribution is supported by the observations after point (B), where the average WOB was increased from ~7 klbm to 15 klbm in the final stand, with very little change in average ROP observed after this.

Given the extensive scope of the field tests, across 76 globally-distributed wells, the aforementioned examples constitute a small sub-set of cases where positive impacts on ROP were observed after utilizing the optimization system's advised drilling parameters. Further field test results demonstrating efficacy at increasing ROP, obtained using the system without integrated safeguards during ultra-deepwater drilling in West Africa, and another offshore well in Malaysia, are available in a previous paper (Al-Riyami et al. 2023).

Impact of ECD safeguarding module on advised drilling parameters

In order for the hole cleaning risk safeguard to be used successfully, sufficiently low prediction errors from the ML model used for downhole ECD estimation needed to be demonstrated. Near-constant offsets between estimated and measured ECD were considered to be less concerning in the scope of safeguarding methodology, which is based on expected changes in ECD rather than the level values. Hence, the methodology has some tolerance to systematic error, and thus verifying that the "random" error component, arising from unpredictable or unobservable changes in drilling conditions for example, was sufficiently

small across a range of independent wells (excluded from data used in the model training process) was a key milestone ahead of integration with the optimization system.

Ahead of deployment in the field, the performance of the ECD model was assessed on observations (13020 in total) from 12 independent wells with downhole ECD measurements available as a reference. This performance was summarized as a residuals distribution, where residuals are defined as the differences between reference and predicted values, shown in Fig. 8. The ideal distribution (uniformly perfect predictions) would have the form of a delta function located at zero, although in practice the goal is to obtain a Gaussian-like distribution, centered on zero (low systematic error), with the lowest possible dispersion (low random error). The authors note that earlier versions of the ECD estimation model reported in this work have been utilized in field operations since 2020, as part of a hole cleaning risk detection and early warning system focused specifically on stuck pipe prevention, with additional results to those presented in this section published in prior works (Robinson et al. 2022b, Payrazyan and Robinson 2023).

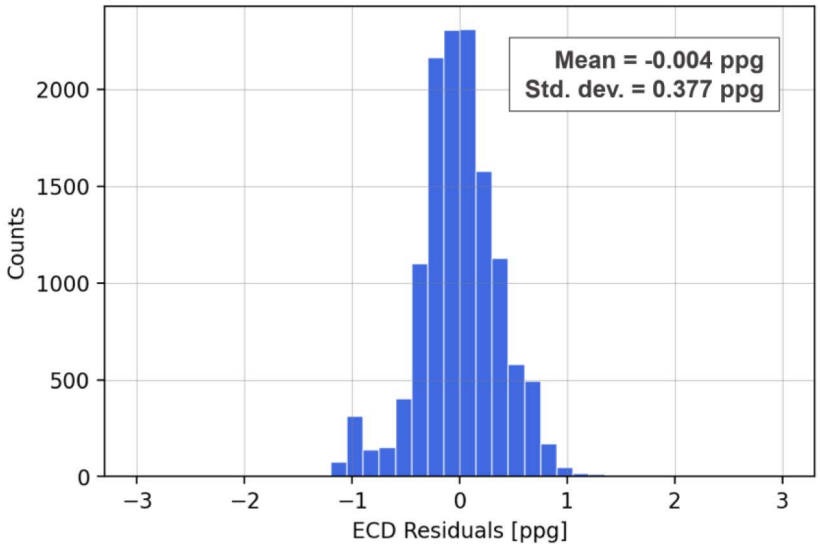

Figure 8—Residuals distribution for the ECD estimation model used within the integrated hole cleaning risk safeguarding utilized in the field. Observations from 12 independent wells, which had not been utilized in model training or validation, were assessed to obtain the histogram.

An illustrative example comparing estimated and reference (measured) ECD values over time is shown in Fig. 9, which represents a ~35 hour time interval from a well drilled in Southeast Asia (not used in training dataset). As visible in Fig. 9(a), the modelled ECD tracked the reference values closely throughout this interval, with Mean Absolute Error (MAE) and Root Mean Squared Error (RMSE) of 0.099 ppg and 0.130 ppg respectively. As a metric, MAE is less affected by outliers than RMSE, hence the RMSE was slightly higher, due to the small tails observed on the residuals distribution in the inset plot Fig. 9(b). Similarly to the 12 well combined test (Fig. 8), this distribution was Gaussian-like in shape and centered close to zero, with a distribution mean of 0.029 ppg and standard deviation of 0.126 ppg, indicating low systematic and random error components in this case. Based on the results presented in Fig. 8 and Fig. 9, the prediction errors observed with the ECD model were low enough to reasonably support usage for scenario modelling in the hole cleaning safeguard.

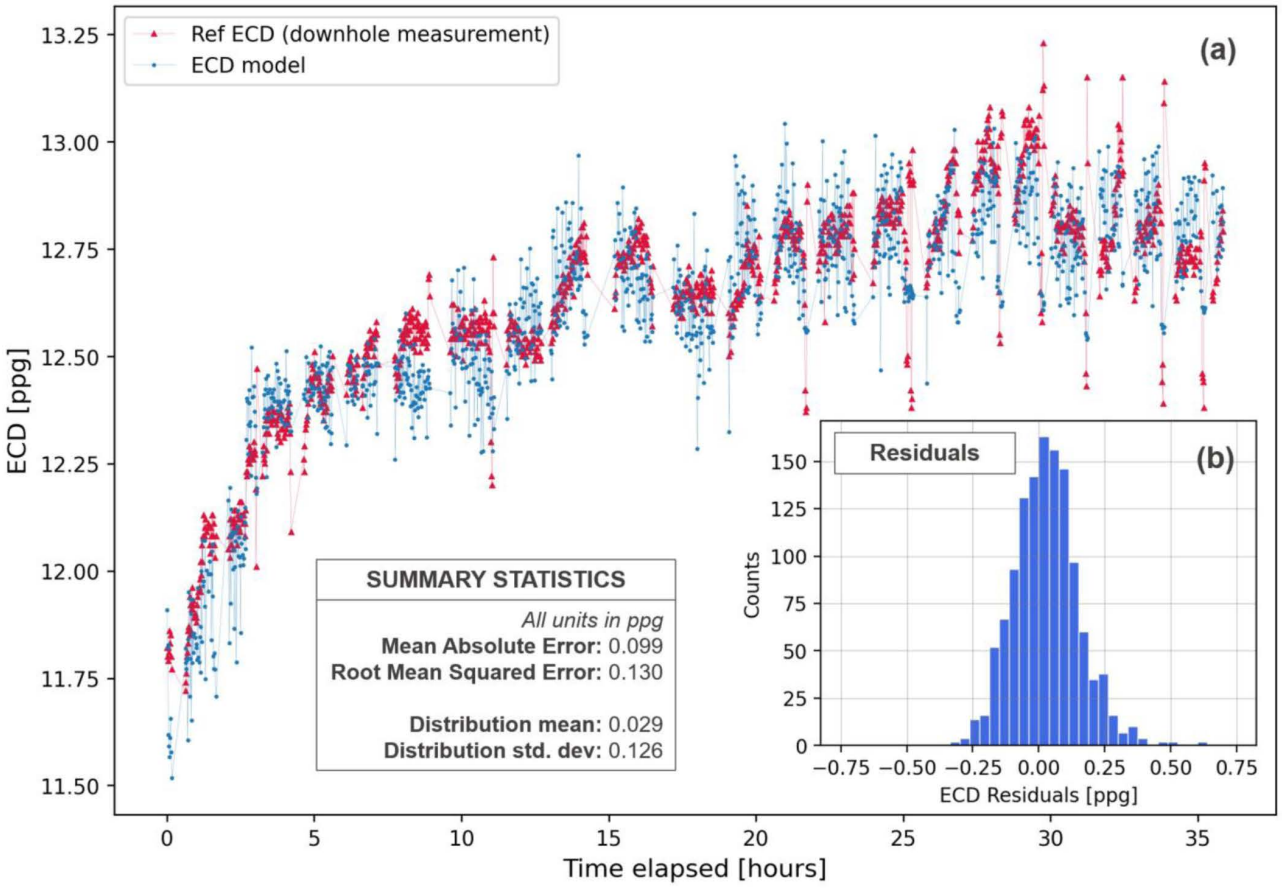

Figure 9—Example interval from a historical well dataset (located in Southeast Asia) comparing downhole ECD measurements, and corresponding estimates for these observations generated by a machine learning model, using only surface data as inputs for inference. The level values for reference and model-estimated ECD are shown in (a), while the corresponding residuals distribution is provided in the inset (b).

The effect of setting more conservative (smaller) ECD change tolerance values on the ROP optimization system's outputs can be seen in Fig. 10, which shows a historical sample drilling period from an ultra-deepwater well in the ofshore West Africa region. Although this analysis was done retrospectively, field test results from using an earlier version of the ROP optimizer, where the rig crew closely adhered to the drilling parameter recommendations, were reported by the authors in a previous paper (Al-Riyami et al. 2023). In Fig. 10(a), the estimated ROP values under different ECD change tolerance scenarios are shown for successive (measured) depth increments, with the baseline ROP estimates (green curve) representing no change to rotary speed or WOB, for the depth increment about to be drilled, from the previously drilled depth increment. The optimized ROP estimates expected from modifying drilling parameters are labelled with the configured ECD change tolerances for each case, one with a very restrictive value (blue curve, 0.01 ppg), and one with a much less conservative setting (red curve, 0.5 ppg). These tolerances were chosen for illustrative purposes, and typically ECD change values in the range 0.3-0.8 ppg are set by default during live operations. The advised rotary speed and WOB values corresponding to the optimized ROP estimates in each scenario are provided in Fig. 10(b) and Fig. 10(c) respectively. For this specific test, the optimizer's allowed search ranges for updated WOB and rotary speed values were set to within ±20% of the baseline values for both variables.

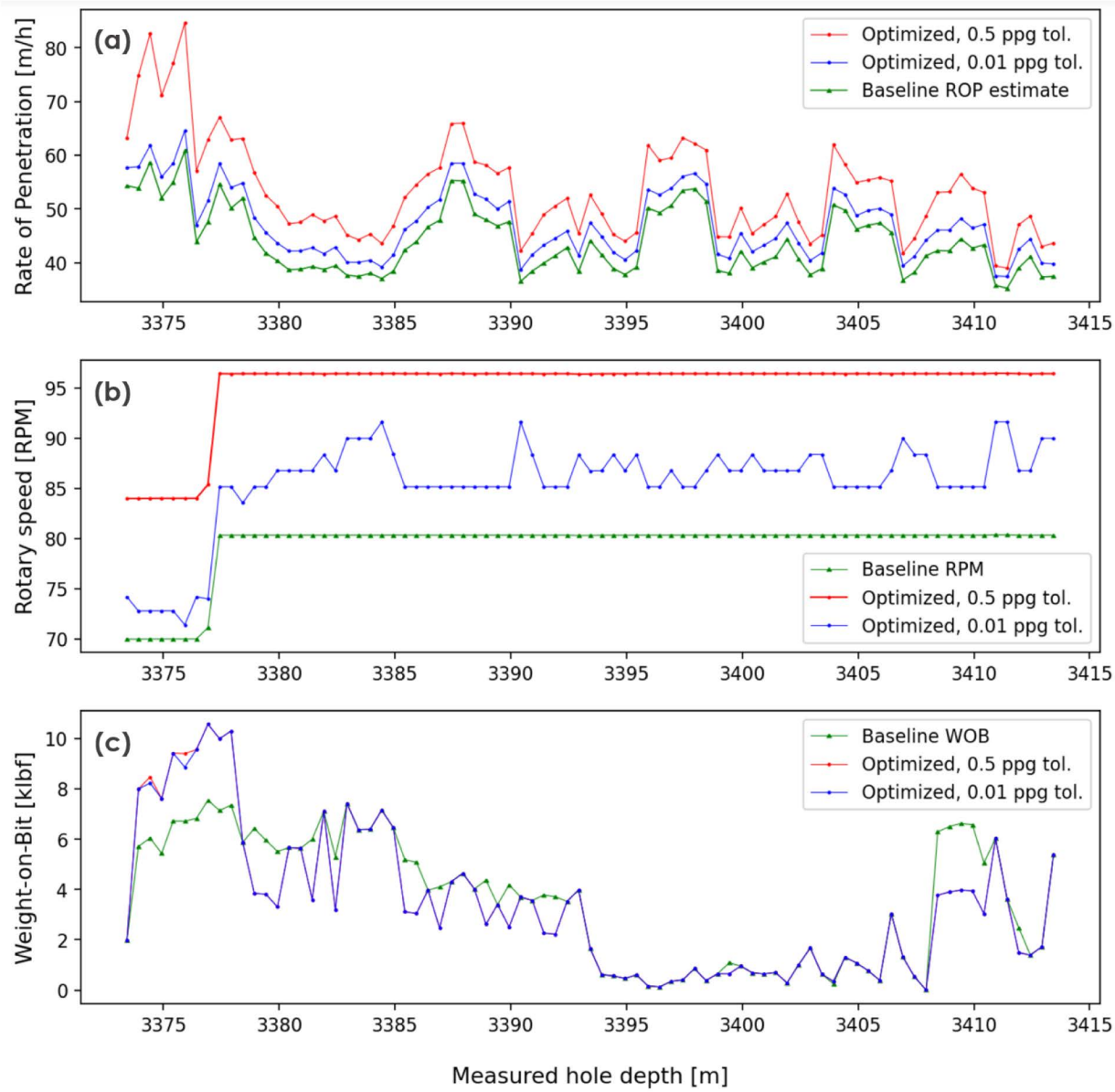

Figure 10—Outputs from testing use of the ROP optimizer with hole cleaning safeguard during a sample drilling period from a historical dataset, an ultra-deepwater well in the ofshore West Africa region. In sub-plot (a), the estimated ROP values at successive depth increments under different scenarios are shown, with the baseline estimate representing no change to rotary speed or WOB, and optimized ROP estimates labelled with the configured ECD change tolerances used to constrain the optimizer. The advised rotary speed and WOB values corresponding to the optimized ROP estimates are provided in sub-plots (b) and (c) respectively.

From a physics standpoint, ECD is expected to increase when drilling at higher penetration rates, due to the generation of additional cuttings per unit time. Hence, the expected behavior for the optimizer under strict ECD change constraints is to limit the final optimized ROP estimated as a result of modifying the drilling parameters, which is indeed observed in Fig. 10(a) for the 0.01 ppg tolerance scenario. These lower estimates for optimized ROP are in turn associated with less aggressive advised drilling parameters, with lower rotary speeds recommended throughout the test interval, and slightly lower WOB values near the beginning. As ECD is expected to be influenced by drillstring rotary speeds (Ahmed 2010), usually increasing with higher RPM, this combined with the heuristic that increased RPM typically leads to higher ROP provides evidence indicating that the behaviors learnt by the ECD model are in line with those expected from a theoretical perspective. Hence, when integrated into the hole cleaning risk safeguard, the machine

learning model was considered to be sufficiently accurate to provide a useful additional constraint to the ROP optimizer.

Since the ECD safeguard was added to the ROP optimization system used in field operations, no pack-off cases have been reported on wells actively utilizing it for drilling parameter advice. This was confirmed by an operator in a public LinkedIn post (Mokhtar 2024). It should be noted that for the majority of these operations (69 of 76 wells), the ROP optimizer ran in conjunction with a dedicated system for detection of stuck pipe risks due to hole cleaning issues, as an additional safety mechanism. Furthermore, the operators' practices to control ROP at certain points while drilling the wells are also expected to have played a role in avoiding hole cleaning issues. Without running a set of field tests specifically dedicated to assessing the hole cleaning safeguard (undesirable for operators who are focused on their core business), without external controls placed on the operations, it is not possible to conclude that the safeguarding system single-handedly prevented issues with poor hole cleaning. However, it is reasonable to state that applying the ROP optimization system with safeguarding modules does not appear to have increased the risk of hole cleaning issues in an observable manner, despite having documented numerous cases of increased ROP after following the drilling parameter advice.

Cases studies of running torsional vibration detection module in field operations

Ahead of field-deployment, the detection model's performance was assessed through analysis of historical well data exhibiting torsional vibration symptoms. This demonstrated that the detector identified stick-slip with high fidelity, achieving a precision of 0.92 on holdout (unseen) drilling data intervals from five wells, with all regions with stick-slip symptoms present in the data identified, even if the estimated stick-slip probability did not exceed the 0.5 threshold at every time step during these regions. The precision statistic quantifies the proportion of estimated stick-slip probabilities exceeding a threshold of 0.5 corresponding to snapshots in time containing torsional vibration symptoms affecting the drill string. This metric provides insights into how often the stick-slip detector wrongly indicates the presence of stick-slip symptoms. The safeguard is robust against brief or isolated misclassifications, due to a requirement for stick-slip symptoms to be present for multiple time-steps in order to prompt any actions. Setting a controllable required minimum time with elevated stick-slip probabilities supports tuneability of how conservatively the safeguarding system behaves, which can be further modified by controlling the probability threshold that must be exceeded to consider the symptoms to require mitigating actions.

An alternative, qualitative, method for assessing the performance of the stick-slip detection system is to review the estimated stick-slip probabilities directly during periods with and without vibration symptoms, where the data was explicitly not used in fitting the ML model; an example time interval containing an onset of torsional vibrations is shown in Fig. 11, which plots (a) surface rotary speed and (b) torque data, alongside (c) the estimated stick-slip probabilities during the same time frame. The light-grey shaded regions indicate time ranges with stick-slip symptoms, starting with the onset of stick-slip identified by the detector just after 2 hours into the sample interval, and followed by two regions with severe torsional vibration symptoms. These shaded areas all contain much higher stick-slip probabilities (in excess of the example threshold of 0.5) compared to the remainder of the sample interval, where stick-slip probabilities are very low at almost all times. Furthermore, the probabilities during the onset of stick-slip symptoms were lower than those estimated in the latter third of the interval, where symptoms were visibly more severe based on the torque data. This is a desirable behavior by the ML model, as it indicates that the stick-slip probabilities provide a useful proxy quantifying the dysfunction severity within an easily interpretable range of [0.0, 1.0]. The history of this metric can thus be monitored over time and depths for retrospective analysis when planning upcoming wells, while the directional variations in stick-slip probability can be used in real-time to assess whether symptoms are worsening, or improving in response to mitigating actions.

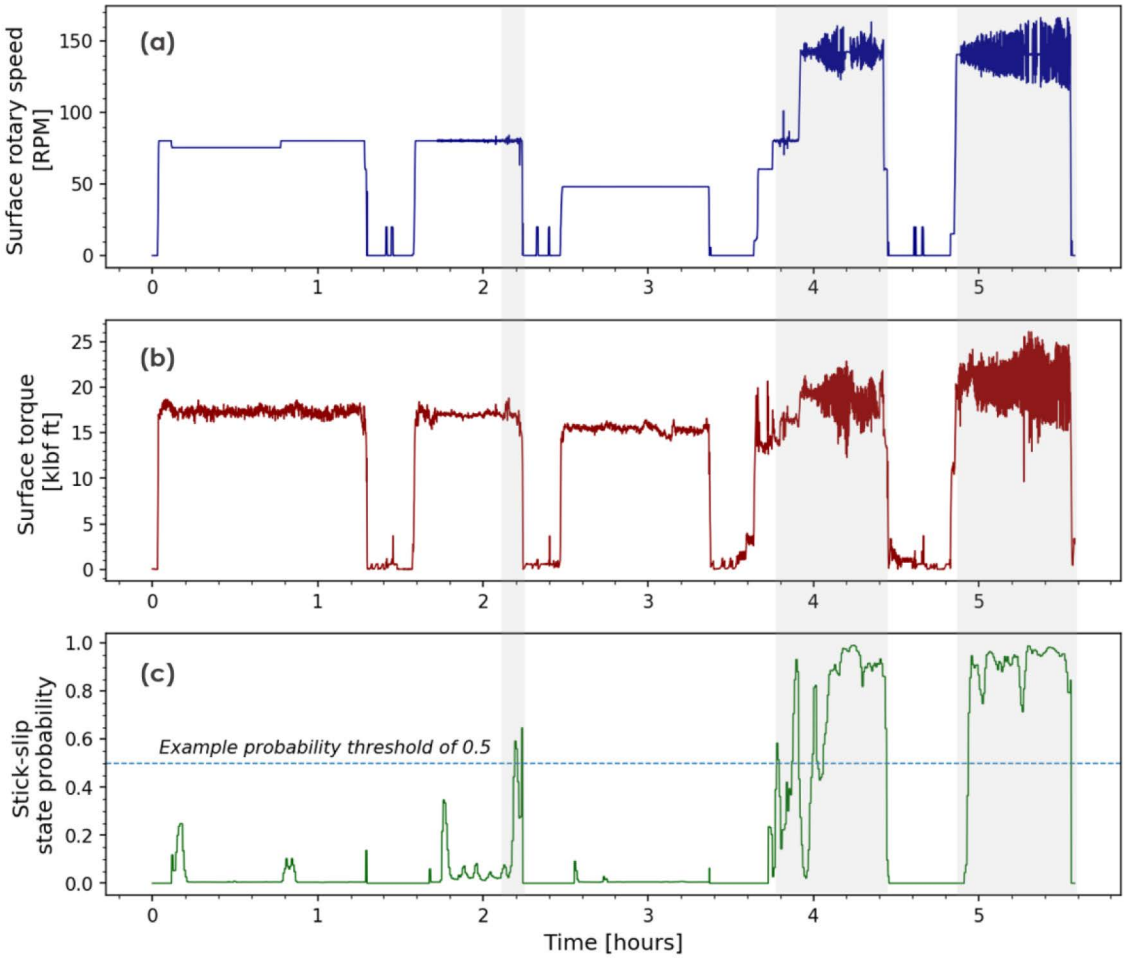

Figure 11—A case from a North Sea well where severe stick-slip issues were encountered. The sub-plots each display a time series, namely (a) surface-measured drill string rotary speed; (b) surface torque measurements; and (c) stick-slip probability estimates providing a quantitative metric relating to vibration severity. The shaded regions indicate time intervals with torsional vibration symptoms present.

Based on these results, the detector was deemed to be sufficiently discriminative between intervals with and without stick-slip symptoms to underpin a safeguarding mechanism against this particular type of drilling dysfunction. Subsequently, the stick-slip detection module was integrated into the ROP optimization system, and the updated system was deployed to field operations, where the end-users based in real-time monitoring centers received the advised drilling parameters and stick-slip probabilities (a proxy for vibration severity) on their displays. Fig. 12 shows a screenshot from a commercial real-time viewer application displaying the stick-slip detector's outputs, in addition to drilling parameter recommendations; this is representative of how the system's outputs were viewed during field operations, although the specifics of the display varied between operators according to their preferred viewer software. The meanings of the various curves are shown via the text annotations. In this particular (illustrative) example, the ROP optimization system was run historically, hence the outputs were not directly acted on, however there were examples where the drilling parameter advice was *coincidentally* followed, for example by increasing rotary speed, indicated by the blue stars added to the screenshot. This recommendation aligns with typical operational practices of increasing rotary speed and decreasing WOB when attempting to mitigate stick-slip issues, despite the core ROP optimizer not directly incorporating the stick-slip severity metric into the scenario modelling steps used to select drilling parameters maximizing ROP within safety constraints.

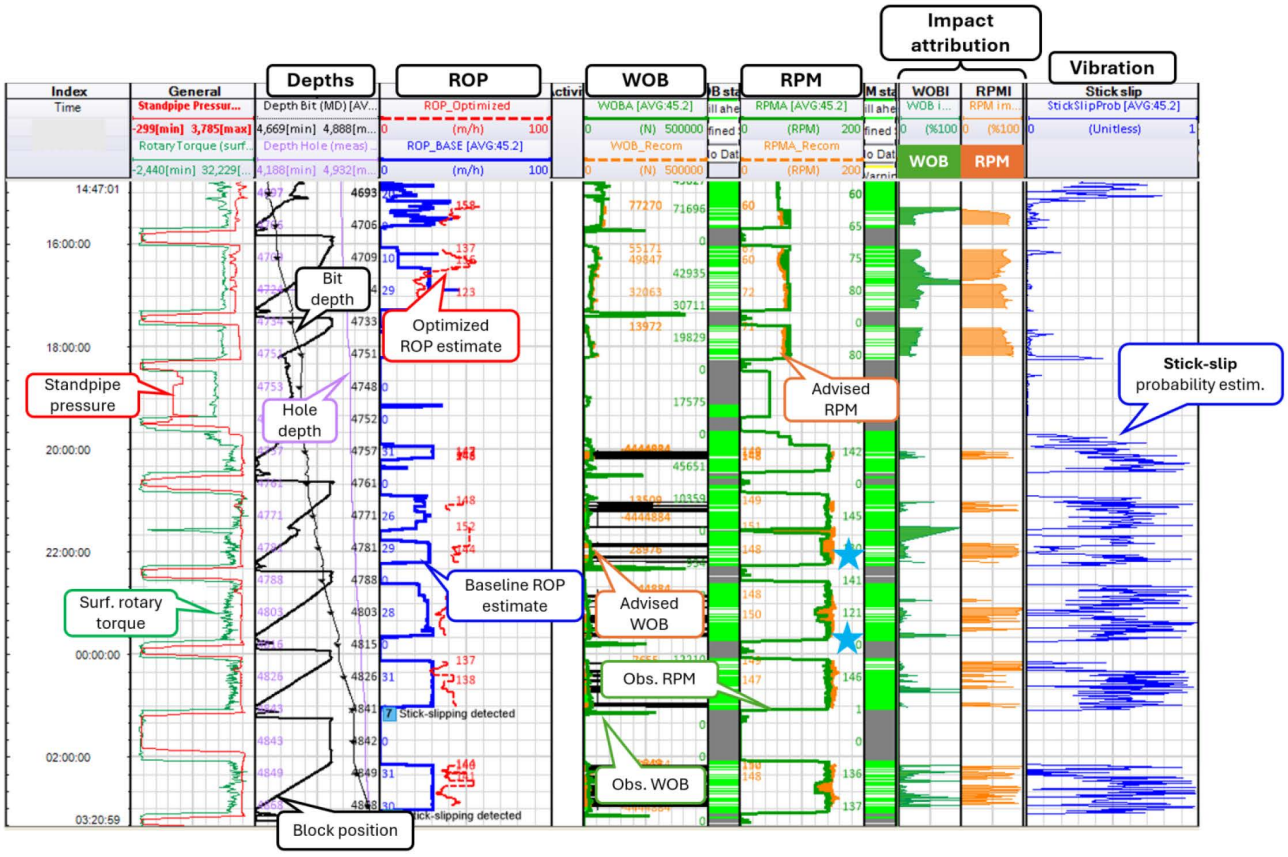

Figure 12—Example screenshot from a commercial real-time viewer application displaying the drilling parameter recommendations from the ROP optimization system, and the stick-slip probability estimates in the right-most track. Stick-slip issues were observed in the torque measurements (green curve, left-most track) during the latter part of the interval, with correspondingly higher stick-slip probabilities estimated during the same time period. Although this figure was created based on historical data for illustrative purposes, the blue stars indicate points in time where the ROP optimizer's recommendations were coincidentally followed by the rig team.

The remainder of this section is focused on example cases from the field where optimizer, supported by both hole cleaning risk and stick-slip safeguards, was utilized effectively in real-time while drilling the wells, which were located in the Middle East and Gulf of Mexico. Furthermore, the system outputs during the live field operations demonstrated that the pre-trained ML model for detecting stick-slip symptoms generalized well to new situations with out-of-sample data, especially considering the model's training data was sourced from wells located in the North Sea, Southeast Asia and South America.

In the first example from a Gulf of Mexico well, vibration issues affecting the drillstring were encountered and correctly identified by the stick-slip detector, as shown in Fig. 13, a screenshot from a WITSML data viewer application. The right-most track in the display plots the variation over time of estimated stick-slip probabilities from the safeguarding module. In this particular well, the system was configured to monitor for stick-slip symptoms, but not to interrupt requests for optimized drilling parameters from the core optimizer, hence advice was generated even during periods with vibration issues. Initially, the drilling occurred without notable stick-slip symptoms, however the probabilities soon began to increase, fluctuating with variation in WOB. The measured ROP (green curve) was observed to be higher in the brief periods with lower stick-slip probabilities, a pattern that was replicated later during the interval at multiple points. Consistently with this observation, areas with higher stick-slip probabilities (for example between 09:40-09:50, and 10:10-10:25) corresponded with reduced ROP and larger fluctuations in the measured surface torque, indicative of reduced drilling efficiency. Furthermore, the trends in stick-slip probability also matched the trends in average ROP quite well, evidence that monitoring the variation in stick-slip

probabilities is indeed a useful proxy for vibration symptom severity. The baseline ROP estimates closely matched the observed ROP in these cases, a sign the ROP model performed well in this area.

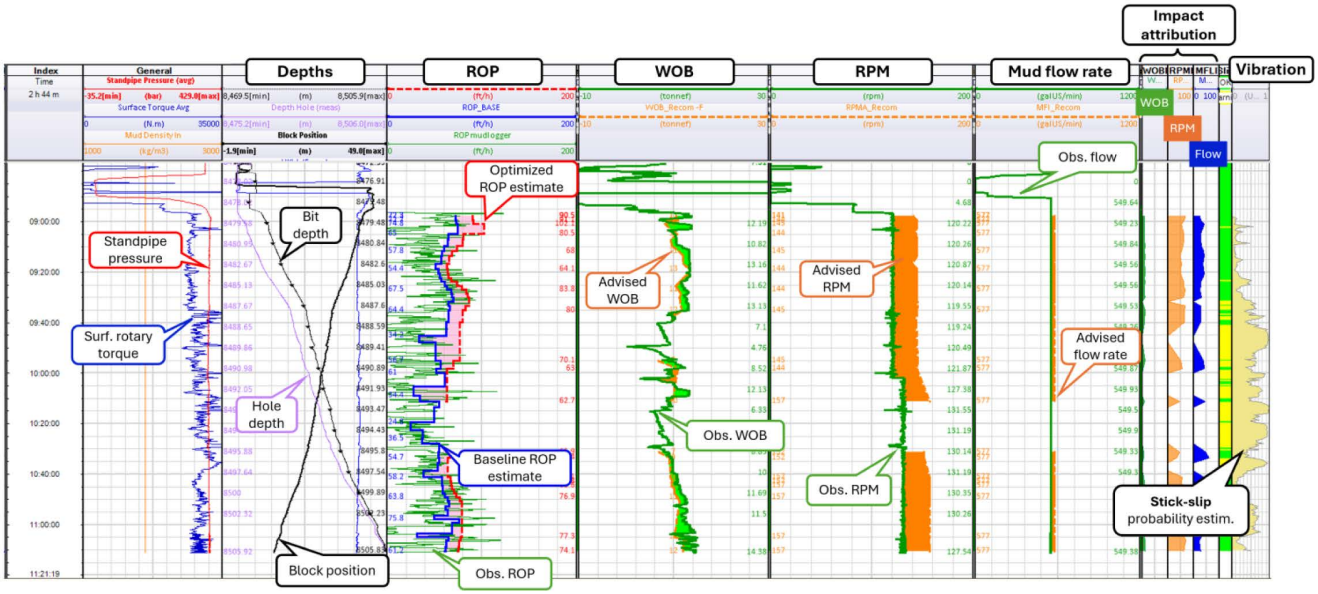

Figure 13—An example from field usage of the ROP optimization system with torsional vibration safeguard on a Gulf of Mexico well, with outputs displayed in a 3rd party commercial viewer application. The right-most track of the display indicates the estimated stick-slip severity.

The drilling parameter advice generated by the ROP optimizer was also consistent with good operational practices in this scenario; during the onset of vibration symptoms, the system recommended reduced WOB and increased rotary speed and mud flow rates. Small reductions in WOB during this interval coincided with increased ROP, for example between 09:20 – 09:25. After increasing the rotary speed, initially higher ROP was observed, although this fluctuated over large amplitudes between 10:05–10:10 after increasing the WOB slightly above the recommended level, as indicated by the light green shaded region in the WOB track between the orange (advised) and green (observed) WOB curves. Higher stick-slip probabilities were again estimated in this time frame. After observing the ROP fluctuation, the WOB was then lowered again. While maintaining higher RPM, the WOB was gradually increased, lowered briefly once more around 10:30 (again coinciding with higher stick-slip probabilities), before continuing the gradual increase. Once again, towards the end of the interval, the optimization system recommended to lower WOB to a perceived optimum around 10 tonne f, slightly below the observed values of ~13 tonne f, while further increasing RPM. Although the stick-slip probabilities remained somewhat elevated around 0.5–0.6 near the end of the displayed time range, these were lower than the values earlier on (midway through) ranging between 0.6–1.0, where the average ROP was lowest.

The remaining case studies discussed in this section refer to wells located in the Middle East. The first of these, located in Oman, is presented in Fig. 14, where stick-slip symptoms of varying severity were observed throughout the interval in the screenshot. As with the previous scenario, in this case the optimization system was configured to continue requests for drilling parameter advice during periods with high estimated stick-slip probabilities. Even without the safeguard actively modifying the optimizer's behavior, the advised parameters again generally corresponded well with standard practices for mitigating stick-slip, with recommendations to slightly reduce WOB, and increase rotary speed, although in this case these were not actively followed by the rig crew, and both WOB and rotary speeds were mostly kept approximately constant within the scope of each stand. In fact, the main RPM change (a reduction) occurred near the end of the first visible stand; after stick-slip probabilities had increased, WOB was reduced and

higher ROP was observed alongside falling stick-slip probabilities. Once the RPM was reduced however, stick-slip probabilities again increased, and ROP decreased again.

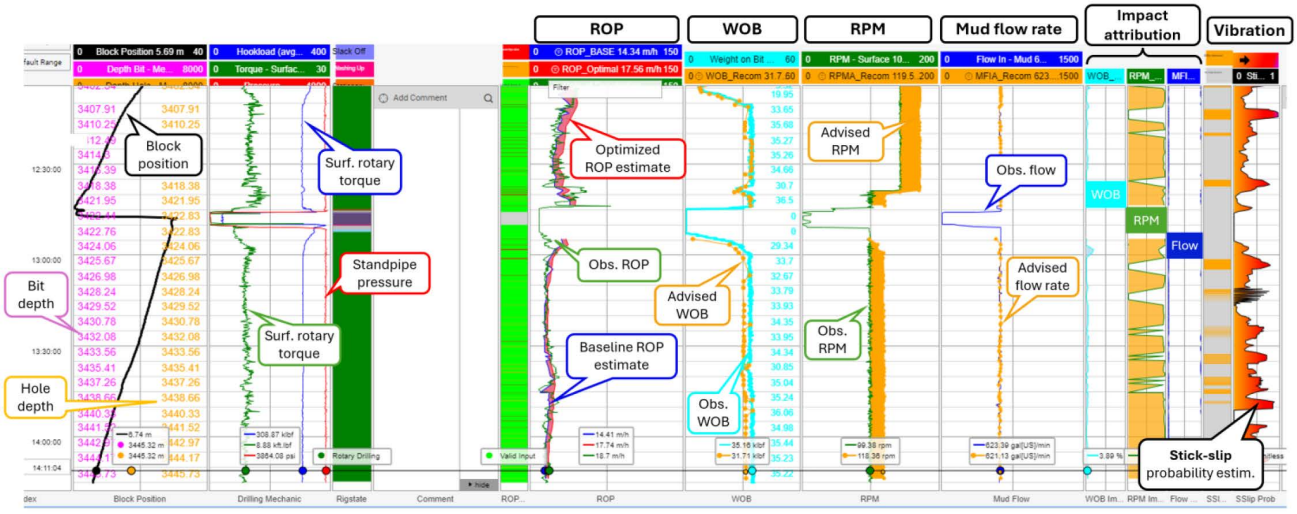

Figure 14—An example from field usage of the ROP optimization system with the (torsional) vibration risk detection system in the Middle East (Oman), with outputs displayed in a third-party commercial viewer application. The right-most track of the display indicates the estimated stick-slip severity. Meanings of the other curves are indicated using the color-coded annotations.

The second Middle Eastern well case study is shown in Fig. 15, where unlike in the previous two cases, the optimization system was configured to pause issuance of drilling parameter advice during periods with stick-slip probabilities exceeding 0.5. During the shaded region marked with point (A), towards the end of the interval with higher WOB values, stick-slip probabilities exceeded the threshold, and drilling parameter advice was not provided. A text message was posted to the comment track notifying the user that stick-slip symptoms had been detected. During the grey-shaded region, the ROP (grey curve) was observed to fall sharply. The rig crew reduced the WOB and increased rotary speed at point (B), and a corresponding reduction in stick-slip probability was observed, with a brief increase in ROP visible at point (B). Around point (C) where WOB was relatively low, the optimizer's advice was to increase WOB by ~10%, which was implemented while maintaining the higher rotary speed, with a clear increase in ROP observed at point (D), from ~45 m/h to an average ROP of ~75 m/h until the end of the stand. During this final few meters of drilling at a higher rate, the stick-slip probabilities remained below the threshold, at values in the range of 0.2-0.3, acting as a secondary indicator of drilling efficiency.

In the final Middle Eastern case study, the ROP optimization system was once again set up to allow drilling parameter recommendations to be issued while high stick-slip probability estimates were provided. As can be seen in Fig. 16 in the shaded region marked with point (A), once the bit tagged the hole-bottom, WOB was increased to ~25 klbf, and stick-slip probabilities rapidly increased. Recommendations to increase rotary speed and slightly reduce WOB from during the shaded interval were actioned at point (B), with a reduction in stick-slip probability observed in response. Note that the after reducing WOB, the optimizer recommended a small increase in WOB, which was implemented at point (C), where further recommendations to increase WOB were issued, and again actioned. Clear ROP increases were observed following the second WOB and RPM increases, which was maintained at an average of ~60 m/h for the remainder of the stand, compared to ~40 m/h earlier on. During this same period, low stick-slip probabilities were provided, suggestive of higher drilling efficiency, as was the case in the latter part of Fig. 15.

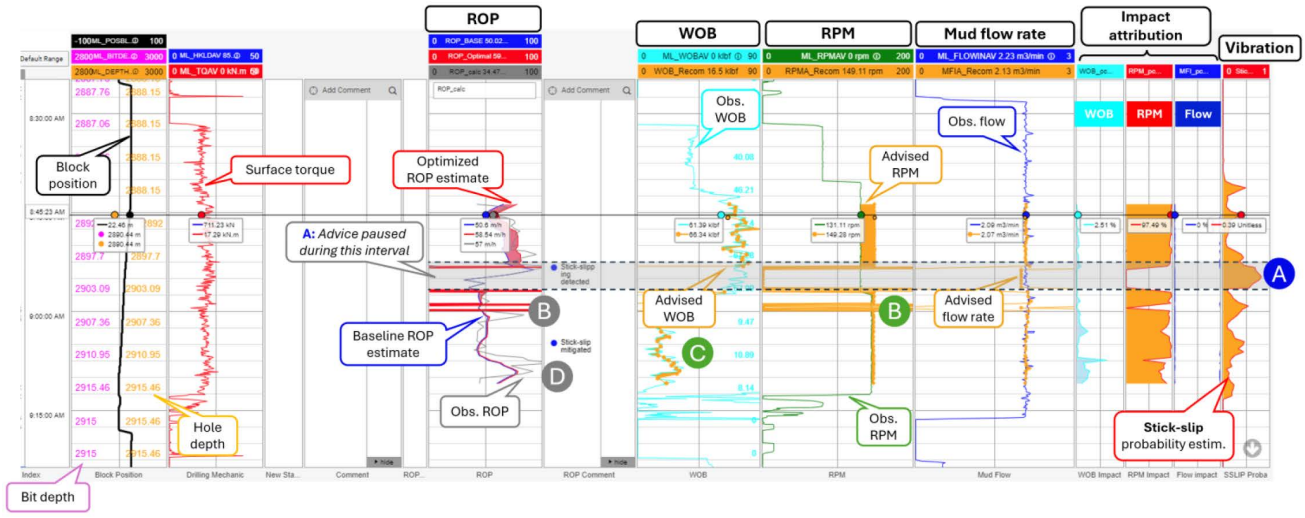

Figure 15—Case study from drilling operation in the Middle East, where the meanings of the curves are indicated by the annotations. Stick-slip symptoms were identified by the reactive safeguarding module at point (A), and drilling parameter advice was paused during the shaded region, where reduced drilling efficiency and lower ROP were observed. The WOB was reduced, and the stick-slip severity metric reduced such that parameter advice resumed, and recommendations to increase RPM and slightly increase WOB were implemented at points (B) and (C). Following these changes, increased ROP was observed at points (B) and (D) shortly following (C).

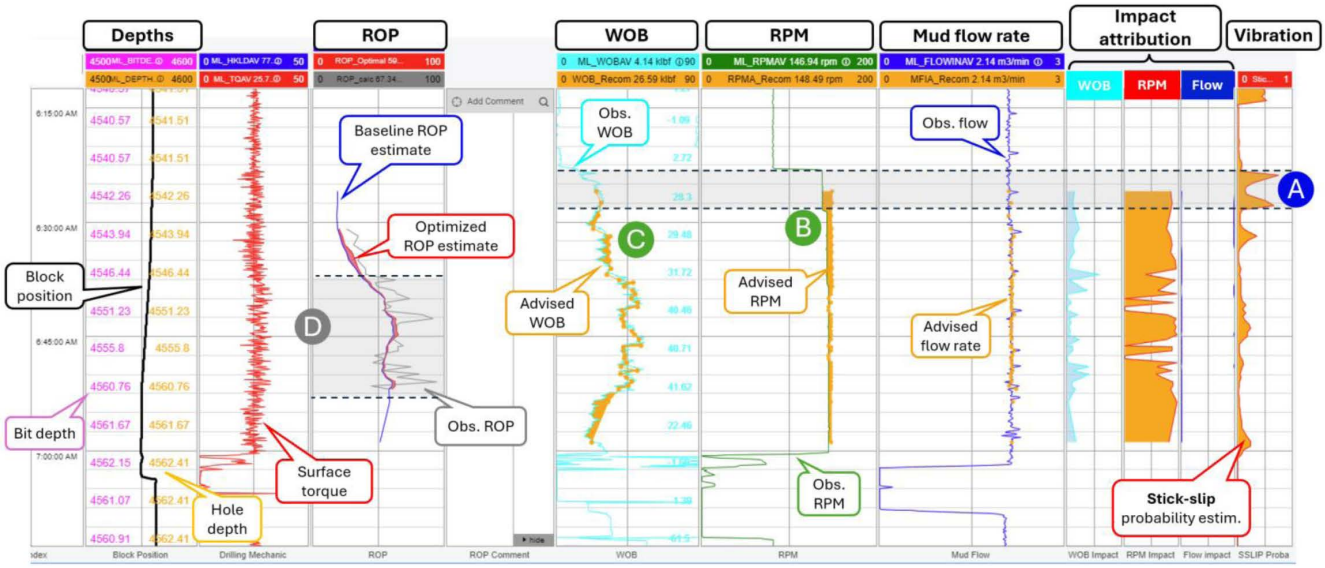

Figure 16—Example from a drilling operation in the Middle East. Following some torsional vibration symptoms in the shaded period (A), both rotary speed and WOB recommendations were followed at points (B) and (C) respectively, with increased ROP observed during the period following the changes, as indicated during the shaded period (D).

In summary, many cases where the stick-slip safeguard provided value were documented during the field tests, with only a select sample presented in this work for the brevity's sake. The safeguarding module was successfully utilized by monitoring teams with conservative setups where drilling parameter advice was paused during areas with vibration symptoms and notification messages issued to users, and also with a configuration to tolerate a degree of stick-slip and continue to issue recommendations. When providing parameter advice during periods with vibration issues, the optimal parameters found using the ROP ML model aligned well with standard good practices for mitigating stick-slip symptoms, despite not being explicitly programmed to do so, This suggests that this was a learned behavior from the ROP model's training dataset, which did include some drilling scenarios with vibration problems, although this information was not explicitly provided to the regression model as an input. Lastly, the most important

proof of efficacy required was documented scenarios where actioning the drilling parameter advice led to increased ROP and drilling efficiency, while factoring in the estimated stick-slip severity indicated by the symptom probabilities; this was demonstrated on numerous occasions during field-usage.

Conclusions

The ROP optimization system with integrated hole cleaning risk and stick-slip safeguards has been actively utilized in the field, on a total of 76 wells at the time of writing, with numerous documented cases where ROP increases were achieved from implementing the advised drilling parameters at the rig. Importantly, no pack-off incidents were reported during these drilling operations, meeting the key objective of the hole cleaning risk safeguard based on modelling ECD for different candidate combinations of drilling parameters, and the estimated ROP values corresponding to these. The stick-slip symptom detection system's effectiveness has been shown to generalize to out-of-sample (new and unfamiliar) wells during field operations, allowing the ROP optimizer's objective to be optionally altered from increased ROP to alerting monitoring teams to facilitate steps to mitigate the torsional vibration issues.

Acknowledgements

The authors thank colleagues Glenn Thomas Folkvoord, Dalila Gomes and Serafima Schaefer for their contributions to this work, particularly for documenting case studies from the field usage of the ROP optimization system.

References

Abdelgawad, K. Z., Elzenary, M., Elkatatny, S.et al. 2019. "New approach to evaluate the equivalent circulating density (ECD) using artificial intelligence techniques", *J Petrol Explor Prod Technol* **9**, 1569–1578 DOI: https://doi.org/10.1007/s13202-018-0572-y

Ahmed, R., Enfis, M., Kheir, H.et al. 2010. "The Effect of Drillstring Rotation on Equivalent Circulation Density: Modeling and Analysis of Field Measurements". Paper presented at the SPE Annual Technical Conference and Exhibition, Florence, Italy, September 2010. Paper Number: SPE-135587-MS. DOI: https://doi.org/10.2118/135587-MS

Alkinani, H. H., Al-Hameedi, A. T., Dunn-Norman, S.et al. 2019. "Data-Driven Neural Network Model to Predict Equivalent Circulation Density ECD." Presented at the SPE Gas & Oil Technology Showcase and Conference, Dubai, UAE, October 2019. DOI: https://doi.org/10.2118/198612-MS

Al-Riyami, N., Revheim, O., Robinson, T. S.et al. 2023. "Drilling in the Digital Age: Case Studies Of Field Testing A Real-time ROP Optimization System Using Machine Learning". Paper presented at the SPE/IADC Middle East Drilling Technology Conference and Exhibition, Abu Dhabi, UAE, May 2023. Paper no. SPE-214521-MS. DOI: https://doi.org/10.2118/214521-MS

Al Saihati, A.et al. 2021(a). "A Statistical Machine Learning Model to Predict Equivalent Circulation Density ECD while Drilling, Based on Principal Components Analysis PCA". DOI: 10.2118/202101-MS.

Al Saihati, A., Elkatatny, S. and Abdulraheem, A. 2021(b). Real-Time Prediction of Equivalent Circulation Density for Horizontal Wells Using Intelligent Machines, *ACS Omega 2021* **6** (1), 934–942, DOI: 10.1021/acsomega.0c05570

Batruny, P., Yahya, H., Omar, A.et al. 2019. "Drilling in the Digital Age: An Approach to Optimizing ROP Using Machine Learning", Abu Dhabi International Petroleum Exhibition & Conference, SPE-197157-MS. DOI: https://doi.org/10.2118/197157-MS

Benzine, A., El Khair, A., Buiting, S.et al., 2024. "AI-Automated Drilling RTOC with ML and Deep Learning Anomaly Detection Approach." Paper presented at the ADIPEC, Abu Dhabi, UAE, November 2024. Paper Number: SPE-222517-MS. DOI: https://doi.org/10.2118/222517-MS

Fernandéz Berrocal, M., Cao, J. and Sui, D. 2022, "Evaluation and Interpretation on Data Driven ROP Models From Engineering Perspectives", Proceedings of ASME 2022 41st International Conference on Ocean, Offshore and Arctic Engineering, Hamburg, Germany, June 2022. OMAE2022-78752. DOI: https://doi.org/10.1115/OMAE2022-78752

Chen, T. and Guestrin, C. 2016. "XGBoost: A Scalable Tree Boosting System". In Proceedings of the 22nd ACM SIGKDD International Conference on Knowledge Discovery and Data Mining (KDD '16). Association for Computing Machinery, New York, NY, USA, 785–794. DOI: https://doi.org/10.1145/2939672.2939785

Cao, J., Ren, H. and Sui, D. 2022. "Global Optimization Workflow for Offshore Drilling Rate of Penetration With Dynamic Drilling Log Data", Proceedings of ASME 2022 41st International Conference on Ocean, Offshore and Arctic Engineering, Hamburg, Germany, June 2022. OMAE2022-79747. DOI: https://doi.org/10.1115/OMAE2022-79747

Elahifar, B. 2024. "Real-Time Artificial Intelligence-Enhanced Machine Learning Technique for Accurate Drilling Parameter Prediction and Optimization." Paper presented at the SPE Annual Technical Conference and Exhibition, New Orleans, Louisiana, USA, September 2024. DOI: https://doi.org/10.2118/220914-MS

Erge, O., Özbayoğlu, M., Özbayoğlu, E. 2022. "A Deep Learning Model for Rate of Penetration Prediction and Drilling Performance Optimization Using Genetic Algorithm", Proceedings of ASME 2022 41st International Conference on Ocean, Offshore and Arctic Engineering, Hamburg, Germany, June 2022. OMAE2022-79623. DOI: https://doi.org/10.1115/OMAE2022-79623

Gamal, H., Abdelaal, A., and Elkatatny, S. 2021. Machine Learning Models for Equivalent Circulating Density Prediction from Drilling Data, *ACS Omega 2021* **6** (41), 27430–27442, DOI: 10.1021/acsomega.1c04363

Gupta, S., Chatar, C., and Celaya, J. R. 2019. "Machine Learning Lessons Learnt in Stick-Slip Prediction." Paper presented at the Abu Dhabi International Petroleum Exhibition & Conference, Abu Dhabi, UAE, November 2019. DOI: https://doi.org/10.2118/197584-MS

Hai, W., He, Y., Li, Y.et al. 2024. "Multi-element drilling parameter optimization based on drillstring dynamics and ROP model", *Geoenergy Science and Engineering*, Vol. **244**, 2025, 213460, ISSN 2949-8910. DOI: https://doi.org/10.1016/j.geoen.2024.213460.

Jiao, S., Li, W., Li, Z.et al. 2024. "Hybrid physics-machine learning models for predicting rate of penetration in the Halahatang oil field, Tarim Basin". *Scientific Reports* **14**, 5957 (2024). DOI: https://doi.org/10.1038/s41598-024-56640-y

Junca Rivera, D. A., Bohorquez Gutierrez, J. R., Dontsova, E.et al. 2022. "How Deep Learning can Provide Consistent Improvement on ROP Through Different Drilling Environments". Paper presented at the IADC/SPE International Drilling Conference and Exhibition, Galveston, Texas, USA, March 2022. Paper Number: SPE-208743-MS. DOI: https://doi.org/10.2118/208743-MS

Kamel, J. M. and Yigit, A. S. 2014. "Modeling and analysis of stick-slip and bit bounce in oil well drillstrings equipped with drag bits", *Journal of Sound and Vibration*, Vol. **333**, Issue 25, 2014, Pages 6885–6899, ISSN 0022-460X. DOI: https://doi.org/10.1016/j.jsv.2014.08.001.

Ledgerwood, L. W., Hoffmann, O. J., Jain, J. R.et al. 2010. "Downhole Vibration Measurement, Monitoring, and Modeling Reveal Stick/Slip as a Primary Cause of PDC-Bit Damage in Today." Paper presented at the SPE Annual Technical Conference and Exhibition, Florence, Italy, September 2010. Paper Number: SPE-134488-MS. DOI: https://doi.org/10.2118/134488-MS

Millan, E., Ringer, M., Boualleg, R. and Li, D. 2019. "Real-Time Drillstring Vibration Characterization Using Machine Learning." Paper presented at the SPE/IADC International Drilling Conference and Exhibition, The Hague, The Netherlands, March 2019. DOI: https://doi.org/10.2118/194061-MS

Mokhtar, T.S. 2024. *LinkedIn.* Posted Friday 12 January 2024 07:29:32 GMT (UTC). URL: https://www.linkedin.com/posts/tsshahrilmokhtar_ddaa-activity-7151475271483711488-Xy_k/

Nautiyal, A. and Kumar Mishra, A. 2023. "Machine Learning Application in Enhancing Drilling Performance". *Procedia Computer Science*, Volume **218**, (2023), Pages 877–886, ISSN 1877-0509. DOI: https://doi.org/10.1016/j.procs.2023.01.068.

Payrazyan, V.K. and Robinson, T.S., 2023. "Leveraging Targeted Machine Learning for Early Warning and Prevention of Stuck Pipe, Tight Holes, Pack Offs, Hole Cleaning Issues and Other Potential Drilling Hazards". Paper presented at Offshore Technology Conference, May 2023, Houston, TX, USA. OTC-32169-MS. DOI: https://doi.org/10.4043/32169-MS

Pavone, D. R., and J. P.Desplans. 1994. "Application of High Sampling Rate Downhole Measurements for Analysis and Cure of Stick-Slip in Drilling." Paper presented at the SPE Annual Technical Conference and Exhibition, New Orleans, Louisiana, September 1994. DOI: https://doi.org/10.2118/28324-MS

Robertson, R., Deans, A., Singh, K.et al. 2023. "Field Test Results for Real-time ROP Optimization Using Machine Learning and Downhole Vibration Monitoring - A Case Study". Paper presented at the SPE/IADC International Drilling Conference and Exhibition, Stavanger, Norway, March 2023. Paper Number: SPE-212568-MS. DOI: https://doi.org/10.2118/212568-MS

Robinson, T.S., Batruny, P., Gomes, D.et al. 2022(a). "Successful Development and Deployment of a Global ROP Optimization Machine Learning Model", Offshore Technology Conference Asia, Kuala Lumpur, Malaysia, March 2022. OTC-31680-MS. DOI: https://doi.org/10.4043/31680-MS

Robinson, T. S., Gomes, D., Meor Hashim, M. M. H.et al. 2022(b). "Real-time Estimation Of Downhole Equivalent Circulating Density (ECD) Using Machine Learning And Applications". Paper presented at SPE/IADC

International Drilling Conference and Exhibition, March 2022, Galveston, TX, USA. SPE-208675-MS. DOI: https://doi.org/10.2118/208675-MS

Robinson, T.S., Revheim, O. 2023. "Automated Detection of Rig Events From Real-time Surface Data Using Spectral Analysis and Machine Learning". Forthcoming paper at SPE/IADC International Drilling Conference and Exhibition, March 2023, Stavanger. SPE-212481-MS. DOI: https://doi.org/10.2118/212481-MS

Robnett, E. W., Hood, J. A., Heisig, G., and Macpherson, J. D. 1999. "Analysis of the Stick-Slip Phenomenon Using Downhole Drillstring Rotation Data." Paper presented at the SPE/IADC Drilling Conference, Amsterdam, Netherlands, March 1999. DOI: https://doi.org/10.2118/52821-MS

Saadeldin, R., Gamal, H. and Elkatatny, S. 2023. "Machine Learning Solution for Predicting Vibrations while Drilling the Curve Section", *ACS Omega 2023* **8** (39), 35822–35836, DOI: 10.1021/acsomega.3c03413

Safarov, A., Iskandarov, V. and Solomonov, D. 2022. "Application of Machine Learning Techniques for Rate of Penetration Prediction". Paper presented at the SPE Annual Caspian Technical Conference, Nur-Sultan, Kazakhstan, November 2022. Paper Number: SPE-212088-MS. DOI: https://doi.org/10.2118/212088-MS

Sheth, P., Roychoudhury, I., Chatar, C. and Celaya, J. 2022. "A Hybrid Physics-Based and Machine-Learning Approach for Stick/Slip Prediction". Paper presented at the IADC/SPE International Drilling Conference and Exhibition, Galveston, Texas, USA, March 2022. Paper Number: SPE-208760-MS. DOI: https://doi.org/10.2118/208760-MS

Singh, K., Yalamarty, S. S., Kamyab, M.et al. 2019. "Cloud-Based ROP Prediction and Optimization in Real Time Using Supervised Machine Learning", SPE/AAPG/SEG Unconventional Resources Technology Conference, Denver, Colorado, USA, July 2019. URTEC-2019-343-MS. DOI: https://doi.org/10.15530/urtec-2019-343

Singh, K., Yalamarty, S., Cheatham, C.et al., 2021. "From Science to Practice: Improving ROP by Utilizing a Cloud-Based Machine-Learning Solution in Real-Time Drilling Operations". SPE/IADC International Drilling Conference and Exhibition, Virtual, March 2021. SPE-204043-MS. DOI: https://doi.org/10.2118/204043-MS

Singh, K., Siddiqui, F., Braga, D.et al. 2022. "ROP Optimization using a Hybrid Machine Learning and Physics-Based Multivariate Objective Function with Real-Time Vibration and Stick-Slip Filters". IADC/SPE International Drilling Conference and Exhibition, Galveston, Texas, USA, March 2022. SPE-208751-MS. DOI: https://doi.org/10.2118/208751-MS

Singh, K., Haddad, T., Borges, T.et al., 2024. "Cloud-To-Driller's HMI Closed-Loop Drilling Automation: Field Test Results with Machine Learning ROP Optimizer". Paper presented at the IADC/SPE International Drilling Conference and Exhibition, Galveston, Texas, USA, March 2024. Paper Number: SPE-217693-MS. DOI: https://doi.org/10.2118/217693-MS

Srivastava, S. 2022. "An Experimental, Modeling and Machine Learning Based Investigation of Stick-Slip Vibrations", PhD dissertation, University of Oklahoma (2022).

Srivastava, S., Sharma, A., and Teodoriu, C. 2024. "Optimizing sampling frequency of surface and downhole measurements for efficient stick-slip vibration detection", *Petroleum*, Vol. **10**, Issue 1, 2024, Pages 30–38, ISSN 2405-6561, DOI: https://doi.org/10.1016/j.petlm.2023.02.004.

U.S. Energy Information Administration and IHS Markit, 2015. "Trends in U.S. Oil and Natural Gas Upstream Costs", Independent Statistics & Analysis, U.S. Department of Energy. Full-text retrieved 13th November 2024 from U.S. EIA website: https://www.eia.gov/analysis/studies/drilling/pdf/upstream.pdf

Wang, J., Li, C.; Cheng, P. 2024. "Data Integration Enabling Advanced Machine Learning ROP Predictions and its Applications". Paper presented at the Offshore Technology Conference, Houston, Texas, USA, May 2024. Paper Number: OTC-35395-MS. DOI: https://doi.org/10.4043/35395-MS

Yahia, H., Romary, T.; Gerbaud, L.et al. 2024. "Combining Machine-Learning and Physics-Based Models to Mitigate Stick-Slip in Real-Time". Paper presented at the IADC/SPE International Drilling Conference and Exhibition, Galveston, Texas, USA, March 2024. Paper Number: SPE-217750-MS DOI: https://doi.org/10.2118/217750-MS

Zhang, C., Song, X., Liu, Z.et al. 2023. "Real-time and multi-objective optimization of rate-of-penetration using machine learning methods, *Geoenergy Science and Engineering*, Vol. **223**, 211568, ISSN 2949-8910. DOI: https://doi.org/10.1016/j.geoen.2023.211568.